PUBLIC ROADS

A JOURNAL OF HIGHWAY RESEARCH

UNITED STATES DEPARTMENT OF AGRICULTURE
BUREAU OF PUBLIC ROADS

VOL. 11, NO. 1 ▽ MARCH, 1930

RESEARCH HAS RESULTED IN A BETTER UNDERSTANDING OF STRESSES IN CONCRETE BRIDGE SLABS

PUBLIC ROADS

A JOURNAL OF HIGHWAY RESEARCH

UNITED STATES DEPARTMENT OF AGRICULTURE
BUREAU OF PUBLIC ROADS

The reports of research published in this magazine are necessarily qualified by the conditions of the tests from which the data are obtained. Whenever it is deemed possible to do so, generalizations are drawn from the results of the tests, and, unless this is done the conclusions formulated must be considered as specifically pertinent only to the described conditions

TABLE OF CONTENTS

THE BUREAU OF PUBLIC ROADS
Willard Building, Washington, D. C.

REGIONAL HEADQUARTERS
Mark Sheldon Building, San Francisco, Calif.

DISTRICT OFFICES

DISTRICT No. 1. Oregon, Washington, and Montana.
Box 3900, Portland, Oreg.

DISTRICT No. 2. California, Arizona, and Nevada.
Mark Sheldon Building, San Francisco, Calif.

DISTRICT No. 3. Colorado, New Mexico, and Wyoming.
301 Customhouse Building, Denver, Colo.

DISTRICT No. 4. Minnesota, North Dakota, South Dakota, and Wisconsin.
410 Hamm Building, St. Paul, Minn.

DISTRICT No. 5. Iowa, Kansas, Missouri, and Nebraska.
8th Floor, Saunders-Kennedy Building, Omaha, Nebr.

DISTRICT No. 6. Arkansas, Oklahoma, and Texas.
1912 Fort Worth National Bank Building, Fort Worth, Tex.

DISTRICT No. 7. Illinois, Indiana, Kentucky, and Michigan.
South Chicago Post Office Bldg., Chicago, Ill.

DISTRICT No. 8. Louisiana, Alabama, Georgia, Florida, Mississippi, South Carolina, and Tennessee.
Box J, Montgomery, Ala.

DISTRICT No. 9. Connecticut, Maine, Massachusetts, New Hampshire, New Jersey, New York, Rhode Island, and Vermont.
Federal Building, Troy, N. Y.

DISTRICT No. 10. Delaware, Maryland, North Carolina, Ohio, Pennsylvania, Virginia, and West Virginia.
Willard Building, Washington, D. C.

DISTRICT No. 11. Alaska.
Goldstein Building, Juneau, Alaska.

DISTRICT No. 12. Idaho and Utah.
Fred J. Kiesel Building, Ogden, Utah.

COMPUTATION OF STRESSES IN BRIDGE SLABS DUE TO WHEEL LOADS[a]

By H. M. Westergaard, Professor of Theoretical and Applied Mechanics, University of Illinois, Urbana, Ill.

PART I.—INTRODUCTORY STATEMENT AND DEFINITIONS

SLABS IN HIGHWAY bridges must be designed to support wheel loads in addition to the distributed dead loads. The present investigation is limited to the problem of the stresses contributed by the wheel loads, it being assumed that the influences of the uniform loads may be estimated with sufficient accuracy by available methods.[1] E. F. Kelley[2] published in 1926 a study of the influence of the concentrated loads, in the light of available results of tests, and he proposed formulas for computing the bending moments. The present investigation, which is purely analytical, applies directly to the case of homogeneous elastic slabs. They are subject to accurate analysis by mathematical theory of elasticity. Since the reinforced concrete bridge slab may be assumed to act in certain respects approximately as a homogeneous elastic slab, the results found for the homogeneous elastic slab may be applied in forming a judgment as to the proper formulas for design. It is notable that the results of this analysis do not differ widely from those derived by E. F. Kelley from the tests, in the study referred to.
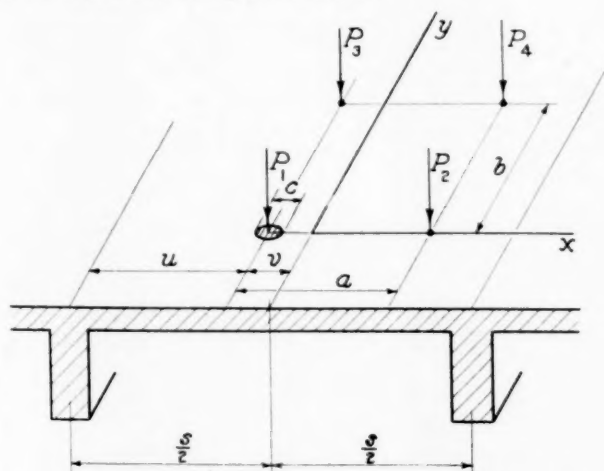

FIGURE 1.—SLAB SUPPORTING WHEEL LOADS

INVESTIGATION OUTLINED

Figure 1 illustrates the problem. The purpose of the analysis is in particular to determine the following effects:

(1) The effect of the load P_1 alone when placed at the center ($v=0$).

(2) The combined effect at the point of application of P_1 produced by the two loads P_1 and P_2 which are separated by the definite distance a, the distance v being chosen so as to produce the greatest possible effect.

(3) The combined effect at the point of application of P_1 produced by the two loads P_1 and P_3, the definite distance b apart, when $v=0$.

(4) The combined effect at the point of application of P_1 produced by the four loads P_1, P_2, P_3, and P_4, which are at the corners of a rectangle with dimensions a and b in the directions of x and y, the distance v being chosen so as to produce the greatest possible effect.

The slab is supported on beams parallel to the direction of y. Most of the computations are based on the assumption that the slab extends sufficiently far in the directions of $+y$ and $-y$ without support by beams in the direction of x to make the influence of edges or beams parallel to the axis of x negligible at the points where the critical stresses exist, thus making it possible for the purpose of analysis to consider the slab to extend infinitely far in the directions of $+y$ and $-y$, without beams or edges in the direction of x. At the same time it will be shown, and illustrated by numerical examples, how the influence of beams in the direction of x may be taken into consideration. When not stated otherwise specifically, the slab will be treated as having simply supported nondeflecting edges along the center lines of the two beams shown in Figure 1. Some computations will be added, however, showing the changes brought about by replacing the simply supported edges by fixed edges. These computations will lead to information about the intermediate cases of partially restrained edges, especially the important case of a continuous slab with several spans in the direction of x.

Each of the four forces P_1, P_2, P_3, and P_4, shown in Figure 1, is the resultant of a wheel pressure which is distributed over a small area. In dealing with the stresses directly under the load P_1, it will be necessary to take into consideration the fact that this load is distributed over an area, but the loads P_2, P_3, and P_4 may be considered as concentrated forces. The load P_1 will be treated as distributed uniformly over a small circle with diameter c. Yet, in expressing effects at some distance from P_1, this load, like the others, may be considered as concentrated at the point of application of the resultant of the pressure.

Two theories of flexure of slabs are used, one of which may be called the ordinary theory, while the other is a special theory. The ordinary theory is based on an assumption which corresponds to the hypothesis of Bernouilli and Navier for beams, that the plane cross section of a beam remains plane and normal to the elastic curve of the beam. The assumption for slabs is that a vertical line drawn through the slab before the bending remains straight and normal to the deflected middle surface after the bending. This assumption applies with satisfactory accuracy to slabs of such proportions as are used commonly in bridges, except for the purpose of expressing the stresses produced by a concentrated load in its immediate vicinity. The difficulty is overcome by use of the special theory in the

following manner.[3] The load is introduced as distributed uniformly over the area of a circle with an "equivalent diameter" c' instead of the true diameter c. By use of the special theory, in particular a solution given by A. Nádai,[4] c' is determined so that the ordinary theory, with c' introduced as the diameter of the circle, leads to the same maximum stress at the bottom of the slab directly under the center of the circle, as does the special theory with the true diameter c introduced. The advantage of this procedure is that after introducing c' all the computations may be made according to the ordinary theory, which, naturally, is much simpler than the special theory. Some of the bending moments computed are to be interpreted, accordingly, as equivalent bending moments. They have the significance that the tensile stresses at the bottom of the slab are computed, in the manner applicable in connection with the ordinary theory, by dividing the bending moment per unit of width of the cross section by the section modulus per unit of width; that is, by $\frac{h^2}{6}$, where h is the thickness of the slab.

The study presented here draws extensively on the work of A. Nádai, published first in papers and later in his book on elastic slabs.[5] In a recent investigation of slabs loaded by concentrated forces M. Bergsträsser[6] obtained a satisfactory experimental verification of Nádai's theory.

The results are presented in formulas, tables, and diagrams.

NOTATION

x, y = horizontal rectangular coordinates. The origin of coordinates is at the center of the span as shown in Figure 1, unless specifically stated otherwise. (The y-axis is moved to the left edge in some particular cases.)

r, θ = horizontal polar coordinates.

z = deflection of slab at point x, y.

a, b, u, v = horizontal distances as shown in Figure 1.

h = thickness of the slab.

c = diameter of circle over the area of which the load P_1 is distributed uniformly.

c' = equivalent diameter of the circle over the area of which the load P_1 is to be considered uniformly distributed in order to make the ordinary theory of flexure of the slab lead to the same maximum tensile stress at the bottom of the slab as does the special theory when the diameter is c.

E = modulus of elasticity of the material of the slab.

μ = Poisson's ratio of the material of the slab. In the numerical computations the value assumed is $\mu = 0.15$.

$N = \dfrac{Eh^3}{12\,(1 - \mu^2)}$ = measure of stiffness of the slab.

P, P_1, P_2, P_3, and P_4 = wheel loads.

w = distributed load per unit of area.

p = load per unit of length distributed over a line.

V_x = vertical shear per unit of width of cross section in a section parallel to the y-axis, positive when acting upward on the part having the larger values of x.

V_y = vertical shear per unit of width of cross section in a section parallel to the x-axis, positive when acting upward on the part having the larger values of y.

M_x, M_y = bending moment in the direction of x or y, respectively, per unit of width of cross section, acting upon a section parallel to the y-axis or x-axis, respectively, positive when it produces compression at the top and tension at the bottom.

M_{xy} = twisting moment in the directions of x and y per unit of width of cross section in sections parallel to the axes of x and y, positive when tending to produce compression at the top in the direction of the line $x = y$.

M'_{xy} = value of M_{xy} in particular cases.

R_x = reaction per unit of length at left edge.

Part II.—DERIVATION OF FUNDAMENTAL FORMULAS

FUNDAMENTAL EQUATIONS OF ORDINARY THEORY OF FLEXURE DERIVED

It appears expedient to introduce the analysis by showing briefly the derivations of the general fundamental equations of the ordinary theory of flexure of slabs.[7]

Figure 2 shows three fundamental types of deformation of an element of the slab. They are produced by the bending moments and twisting moments acting on the element. One may visualize the deformation of the element in the general case by imagining the three types existing in the same element at the same time, superimposed one on another.

Figure 3 shows the total forces and couples acting on a small block of the slab extending through the thickness of the slab. In passing from the face with

coordinate x to that with coordinate $x + dx$, the bending moment per unit of width, M_x, increases at the rate of $\dfrac{\partial M_x}{\partial x}$ by the amount $\dfrac{\partial M_x}{\partial x}\,dx$. The values per unit of width, therefore, may be stated as follows: M_x at the face with the coordinate x; and $M_x + \dfrac{\partial M_x}{\partial x}\,dx$ at the face with the coordinate $x + dx$. The total moments on the width dy, consequently, may be stated as shown in Figure 3: $M_x dy$ at the face with coordinate x; and $(M_x + \dfrac{\partial M_x}{\partial x}\,dx)dy$ at the face with coordinate $x + dx$. Similar explanations apply to the bending moment M_y, the twisting moments M_{xy} and M_{yx}, and the shears V_x and V_y.

[3] Described in a previous paper by the writer, Stresses in Concrete Pavements Computed by Theoretical Analysis, Public Roads, vol. 7, No. 2, April, 1926, p. 25, especially pp. 27, 31, and 32.

[4] A. Nádai, Die Biegungsbeanspruchung von Platten durch Einzelkräfte, Schweizerische Bauzeitung, vol. 76, 1920, p. 257; and his book, Die elastischen Platten, 1925 p. 308.

[5] A. Nádai, Die elastischen Platten, Berlin (Julius Springer), 1925.

[6] M. Bergsträsser, Versuche mit freiaufliegenden rechteckigen Platten unter Einzelkraftbelastung, Forschungsarbeiten auf dem Gebiete des Ingenieurwesens, No. 302, 1928.

[7] These derivations may be found at a number of places in the technical literature. See, for example, A. Nádai, Die elastischen Platten, 1925, p. 20; or the paper by W. A. Slater and the writer, Moments and Stresses in Slabs, Proceedings, American Concrete Institute, vol. 17, 1921, p. 415 (or, National Research Council, Reprint and Circular Series, No. 32).
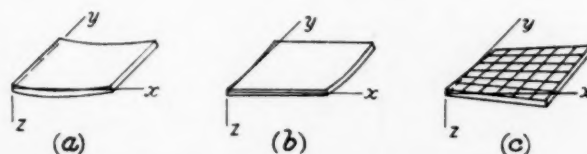

FIGURE 2.—DEFORMATIONS OF ELEMENT OF SLAB, (a) BENDING IN DIRECTION OF x, (b) BENDING IN DIRECTION OF y, (c) TWISTING IN DIRECTIONS OF x AND y
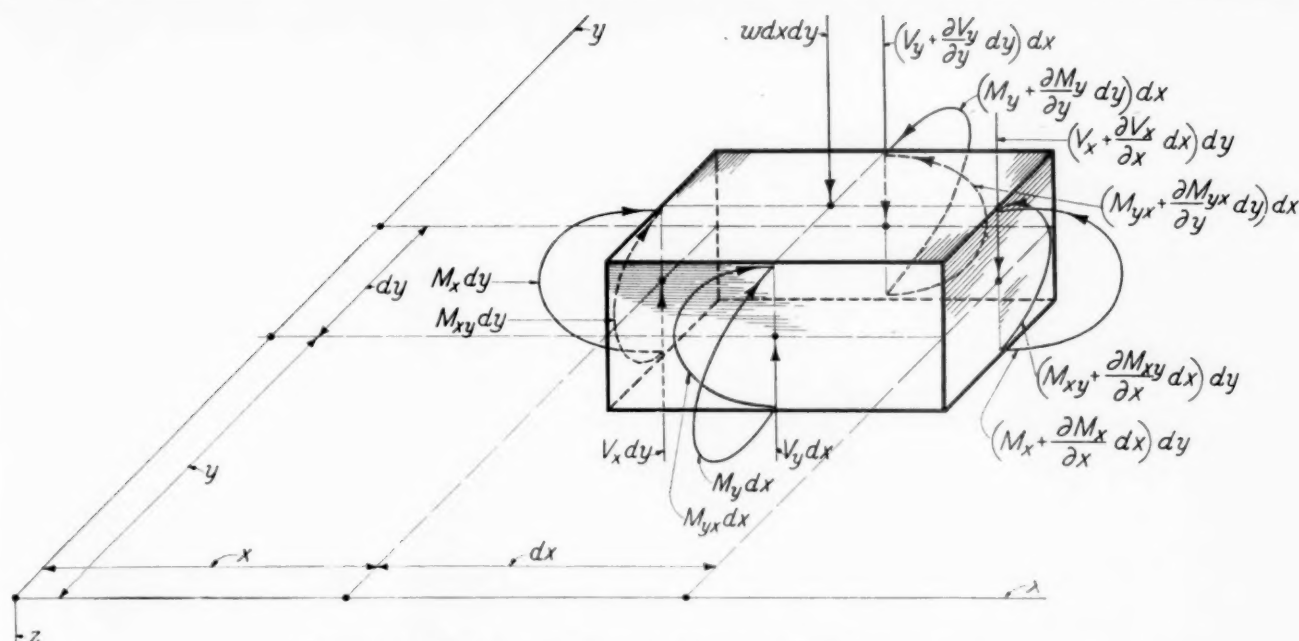
FIGURE 3.—FORCES AND COUPLES ACTING ON ELEMENT OF SLAB

One may write three independent equations of equilibrium of the forces and couples. By equating to zero the sum of the vertical forces, and dividing by $dx\,dy$, one finds

$$\frac{\partial V_x}{\partial x} + \frac{\partial V_y}{\partial y} + w = 0 \quad\text{---------------------}(1)$$

By equating to zero the sum of the moments with respect to an axis through the center of the block, parallel to the y-axis, by discarding the term which is infinitesimal of the third order, $\frac{\partial V_x}{\partial x}\,dx\,dy\cdot\frac{1}{2}dx$, and again dividing by $dx\,dy$ one finds the equation:

$$\frac{\partial M_x}{\partial x} + \frac{\partial M_{yx}}{\partial y} = V_x \quad\text{-------------}(2)$$

The third equation of equilibrium is similar to equation 2, and is obtained by exchanging the symbols x and y in equation 2:

$$\frac{\partial M_y}{\partial y} + \frac{\partial M_{xy}}{\partial x} = V_y \quad\text{-------------}(3)$$

The twisting moments are moments of horizontal shearing stresses in the vertical sections. By applying the law of equality of shearing stresses in perpendicular sections, one finds

$$M_{xy} = M_{yx} \quad\text{-----------------}(4)$$

By substituting the expressions for V_x and V_y, as given in equations 2 and 3, in equation 1, one finds the additional equation of equilibrium,

$$\frac{\partial^2 M_x}{\partial x^2} + 2\frac{\partial^2 M_{xy}}{\partial x\partial y} + \frac{\partial^2 M_y}{\partial y^2} = -w \quad\text{--------}(5)$$

When each straight line drawn vertically through the homogeneous slab before bending remains straight after the bending, the horizontal normal stresses and shearing stresses in the vertical sections will be distributed through the thickness of the slab according to straight-line diagrams, with extreme, equal and opposite values at the top and the bottom and the value zero at the middle. The middle surface of the slab, therefore, is a neutral surface. At the bottom, the tensile stresses σ_x in the direction of x, and σ_y in the direction of y, and the shearing stress τ_{xy} in the directions of x and y are determined as in the case of beams, by dividing the moments by the section modulus, which is $\frac{h^2}{6}$ per unit of width of the section; that is,

$$\sigma_x = \frac{6\,M_x}{h^2}, \sigma_y = \frac{6\,M_y}{h^2}, \tau_{xy} = \frac{6\,M_{xy}}{h^2} \quad\text{------}(6)$$

The next step is to express the relations between the moments and the deformations. The deformations in Figure 2, (a) and (b), are measured by the curvatures, $-\frac{\partial^2 z}{\partial x^2}$ in the direction of x, and $-\frac{\partial^2 z}{\partial y^2}$ in the direction of y, respectively. The deformation in Figure 2 (c) is measured by the twist, $-\frac{\partial^2 z}{\partial x\partial y}$. The bending moment M_x alone, without the action of M_y and M_{xy}, produces a curvature, $-\frac{\partial^2 z}{\partial x^2}$, in the direction of x, which is expressed as in the case of a beam with rectangular cross section of depth h and width equal to one unit, that is, $-\frac{\partial^2 z}{\partial x^2} = \frac{12 M_x}{Eh^3}$. On account of Poisson's ratio, μ, of lateral contraction to longitudinal extension, this curvature will be accompanied by a curvature in the direction of y, equal to $-\mu$ times the curvature in the direction of x. The bending moment M_x produces no twist of the type $-\frac{\partial^2 z}{\partial x\partial y}$. By expressing in a similar manner the effects of the bending moment M_y, one finds the combined effect of the two bending moments,

$$-\frac{\partial^2 z}{\partial x^2} = \frac{12}{Eh^3}\,(M_x - \mu M_y) \quad\text{----------}(7)$$

$$-\frac{\partial^2 z}{\partial y^2} = \frac{12}{Eh^3}\,(M_y - \mu M_x) \quad\text{--------}(8)$$

The effects of the twisting moments M_{xy} may be found by introducing a new system of horizontal rectangular coordinates, x_1, y_1, with the angle $(xx_1)=45°$, so that $x_1=\dfrac{1}{\sqrt{2}}(x+y)$, $y_1=\dfrac{1}{\sqrt{2}}(-x+y)$. When f is any function, one finds

$$\frac{\partial f}{\partial x}=\frac{\partial f}{\partial x_1}\frac{\partial x_1}{\partial x}+\frac{\partial f}{\partial y_1}\frac{\partial y_1}{\partial x}=\frac{1}{\sqrt{2}}\left(\frac{\partial f}{\partial x_1}-\frac{\partial f}{\partial y_1}\right).$$

This result may be written as a statement concerning the operator $\dfrac{\partial}{\partial x}$: Namely $\dfrac{\partial}{\partial x}=\dfrac{1}{\sqrt{2}}\left(\dfrac{\partial}{\partial x_1}-\dfrac{\partial}{\partial y_1}\right)$.

One finds in the same manner, $\dfrac{\partial}{\partial y}=\dfrac{1}{\sqrt{2}}\left(\dfrac{\partial}{\partial x_1}+\dfrac{\partial}{\partial y_1}\right)$, and accordingly, by combining the differential operations:

$$\frac{\partial^2 z}{\partial x \partial y}=\frac{1}{2}\left(\frac{\partial}{\partial x_1}-\frac{\partial}{\partial y_1}\right)\left(\frac{\partial z}{\partial x_1}+\frac{\partial z}{\partial y_1}\right)=\frac{1}{2}\left(\frac{\partial^2 z}{\partial x_1^2}-\frac{\partial^2 z}{\partial y_1^2}\right).$$

The state of moments, $M_x=0$, $M_y=0$, $M_{xy}\neq 0$, is equivalent to the following state of moments in the directions of x_1 and y_1: $M_{x_1}=M_{xy}$, $M_{y_1}=-M_{xy}$, $M_{x_1y_1}=0$. By using these values in equations 7 and 8, with x and y replaced by x_1 and y_1, and then substituting in the expression for $\dfrac{\partial^2 z}{\partial x \partial y}$, one finds

$$-\frac{\partial^2 z}{\partial x \partial y}=\frac{12(1+\mu)}{Eh^3}M_{xy} \quad\text{------}(9)$$

By this method one finds, furthermore, for the same state of moments,

$$\frac{\partial^2 z}{\partial x^2}=\frac{1}{2}\left(\frac{\partial}{\partial x_1}-\frac{\partial}{\partial y_1}\right)^2 z=\frac{1}{2}\left(\frac{\partial^2 z}{\partial x_1^2}-2\frac{\partial^2 z}{\partial x_1 \partial y_1}+\frac{\partial^2 z}{\partial y_1^2}\right)=0,$$

and likewise $\dfrac{\partial^2 z}{\partial y^2}=0$. That is, the twisting moment M_{xy} does not contribute to the curvatures, $-\dfrac{\partial^2 z}{\partial x^2}$ and $-\dfrac{\partial^2 z}{\partial y^2}$.

The three equations, 7, 8, and 9, express therefore the combined effect of the state of bending moments, M_x and M_y, and twisting moments, M_{xy}.

It is expedient to introduce the following quantity, which is a measure of the stiffness of the slab:

$$N=\frac{Eh^3}{12(1-\mu^2)} \quad\text{------------}(10)$$

Using this quantity, one finds, by solving equations 7, 8, and 9 for the moments,

$$M_x=N\left(-\frac{\partial^2 z}{\partial x^2}-\mu\frac{\partial^2 z}{\partial y^2}\right) \quad\text{------}(11)$$

$$M_y=N\left(-\frac{\partial^2 z}{\partial y^2}-\mu\frac{\partial^2 z}{\partial x^2}\right) \quad\text{------}(12)$$

$$M_{xy}=-N(1-\mu)\frac{\partial^2 z}{\partial x \partial y} \quad\text{------}(13)$$

By substituting these expressions in equation 5, one obtains the equation of flexure of the slab, stated by Lagrange in 1811, and frequently named after him,

$$\frac{\partial^4 z}{\partial x^4}+2\frac{\partial^4 z}{\partial x^2 \partial y^2}+\frac{\partial^4 z}{\partial y^4}=\frac{w}{N} \quad\text{------}(14)$$

By introducing the differential operator, known as Laplace's operator for two variables,

$$\Delta=\frac{\partial^2}{\partial x^2}+\frac{\partial^2}{\partial y^2} \quad\text{------------}(15)$$

Lagrange's equation is restated in the simple form,

$$N\Delta^2 z=w \quad\text{------------}(16)$$

The vertical shears are expressed in terms of the deflections by substituting the expressions in equations 11, 12, and 13, in equations 2 and 3. One finds

$$V_x=-N\frac{\Delta z}{\partial x},\quad V_y=-N\frac{\Delta z}{\partial y} \quad\text{------}(17)$$

(a)   (b)
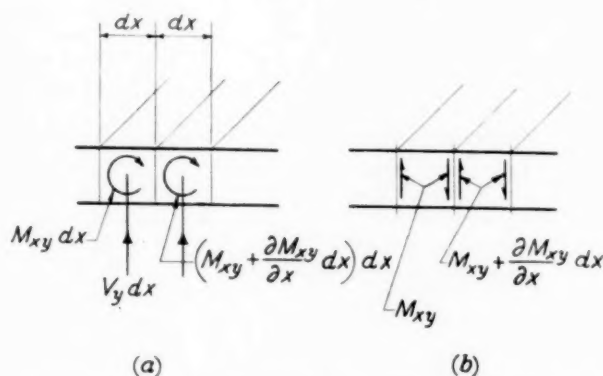
FIGURE 4.—TWISTING MOMENTS AND SHEARS AT EDGE

Figure 4 shows an edge of the slab. The twisting couples in Figure 4 (a) are resultants of horizontal shearing forces. These couples are equivalent to the pairs of vertical forces shown in Figure 4 (b). The two vertical forces at the boundary between the two blocks leave a surplus upward force equal to $\dfrac{\partial M_{xy}}{\partial x}dx$, that is, $\dfrac{\partial M_{xy}}{\partial x}$ per unit of length. This consideration of vertical shears and twisting moments at the edge leads to the theorem given by Kelvin and Tait [5] in 1867: The combination of vertical shears and twisting moments at the edge is equivalent to a combination of vertical forces only, in terms of which the reactions are stated; namely, first, a distributed upward reaction,

$$R_y=V_y+\frac{\partial M_{xy}}{\partial x} \quad\text{------------}(18)$$

secondly, an upward concentrated force at the left end of the edge equal to the value of M_{xy} at that point; and thirdly, a downward concentrated force at the right end of the edge equal to the value of M_{xy} at that point. At an edge parallel to the y-axis, with the slab on the side of the larger values of x one obtains by the same method a distributed upward reaction,

$$R_x=V_x+\frac{\partial M_{xy}}{\partial y} \quad\text{------------}(19)$$

At a rectangular corner formed by the two edges mentioned, each edge furnishes an upward force equal to

[5] Thomson (Lord Kelvin) and Tait, Natural Philosophy, 1867. See arts. 64, 66 in the later editions.

the value of M_{xy} at the corner, giving a total concentrated force equal to $2M_{xy}$.

The problem of the ordinary theory of flexure of the slab is to find a solution of Lagrange's equation 16, satisfying the special conditions existing at the boundary of the area investigated. The boundary conditions are expressed by use of equations 11, 12, 13, 17, 18, and 19.

USE OF INFINITE SERIES EXPLAINED

Consider a simple beam with span s, carrying some concentrated loads and in addition a distributed load, the latter expressed by the function $p = p(x)$, the distance x being measured from the left end. The vertical shear in this beam is a function $V = V(x)$, which changes suddenly at the points of application of the concentrated loads, and which at all other points is governed by the relation,

$$p = -\frac{dV}{dx} \tag{20}$$

Any function V which is obtainable in this manner may be expressed by a Fourier series, which converges toward V except at the points of application of the concentrated loads and at the ends of the beam, of the form

$$V_1 = \sum_{1, 2, \ldots}^{n} c_n \cos \frac{n \pi x}{s} \tag{21}$$

where $c_1, c_2, \ldots c_n, \ldots$ are constants. Assuming that a set of constants exists bringing about the convergence,[9] one may determine the constants by the criterion,

$$\int_0^s (V - V_1) \cos \frac{m \pi x}{s} dx = 0, \ m = 1, 2, \ldots \tag{22}$$

Using the relations,

$$\int_0^s \cos \frac{m \pi x}{s} \cos \frac{n \pi x}{s} dx = \begin{cases} 0 \text{ when } n \neq m \\ \frac{s}{2} \text{ when } n = m \end{cases} \tag{23}$$

one finds, by substituting V_1 from equation 21 in equation 22:

$$c_m = \frac{2}{s} \int_0^s V \cos \frac{m \pi x}{s} dx \tag{24}$$

whereby all the constants $c_1, c_2, \ldots$ may be determined when the function V is known.

By differentiating equation 21 and reversing signs, one obtains a new Fourier series,

$$p_1 = -\frac{dV_1}{dx} = \sum_{1, 2, \ldots}^{n} \frac{n \pi c_n}{s} \sin \frac{n \pi x}{s} \tag{25}$$

which in a special case converges toward p in equation 20 at all points where p does not change suddenly; this special case is that in which all the concentrated loads are zero. If the concentrated loads are not zero, the Fourier series in equation 25 becomes divergent. Yet, integration of the series, with reversal of signs,

reproduces V_1 in equation 21, and further successive integrations lead to expressions for the bending moments, slopes, and deflections in terms of convergent Fourier series. So far as these effects are concerned, the aggregation of individual loads $\frac{n \pi c_n}{s} \sin \frac{n \pi x}{s}$ expressed by the divergent series in equation 25, is equivalent to the complete load on the beam. That is, the series in equation 25, in spite of being divergent, represents the complete load on the beam, consisting of the distributed load $p(x)$, and the concentrated forces.[10]

The series in equations 21 and 25 apply outside the interval $0 < x < s$ when the function V is periodic with period $2s$, and symmetrical with respect to the points $x = 0$ and $x = s$, that is, when $V(x) = V(-x)$, and $V(s + x) = V(s - x)$. The function p_1 has the same period, and is antisymmetrical with respect to the points $x = 0$ and $x = s$, that is, $p_1(x) = -p_1(-x)$, $p_1(s + x) = -p_1(s - x)$. The functions apply then to a continuous beam with simple supports at the points $x = 0, \pm s, \pm 2s \ldots \ldots$
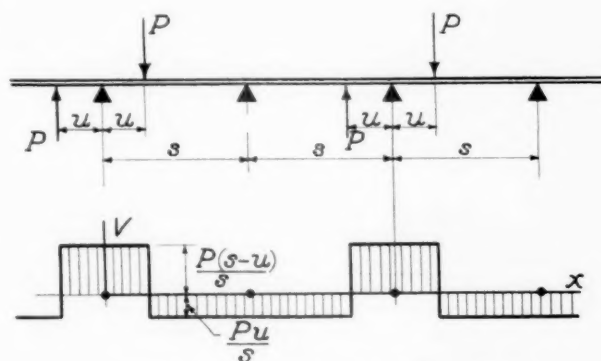
FIGURE 5.—VERTICAL SHEARS IN BEAM

In the case shown in Figure 5 one finds, using equations 24, 21, and 25, and writing V for V_1, and p for p_1:

$$V = \frac{2P}{\pi} \sum_{1, 2, \ldots}^{n} \frac{1}{n} \sin \frac{n \pi u}{s} \cos \frac{n \pi x}{s} \tag{26}$$

$$p = \frac{2P}{s} \sum_{1, 2, \ldots}^{n} \sin \frac{n \pi u}{s} \sin \frac{n \pi x}{s} \tag{27}$$

The latter expression will be used in representing a concentrated load on the slab.

SOLUTION FOR SLAB LOADED BY CONCENTRATED FORCE, EXPRESSED BY INFINITE SERIES

The y-axis is placed temporarily at the left edge of the slab. The edges, at $x = 0$ and $x = s$, are simply supported. The slab extends infinitely far in the directions of $+y$ and $-y$, and is loaded by a single force P at the point $x = u$, $y = 0$. This load will be represented as a load p on the x-axis defined by equation 27.

The function z, representing the deflections in the part of the slab in which y is positive, is defined by the requirement that it must satisfy Lagrange's equation,

---

[9] For proof of the existence of the set of constants bringing about the convergence, see, for example, E. T. Whittaker and G. N. Watson, Modern Analysis, second edition (Cambridge), 1915, p. 161.

[10] The use of divergent Fourier series in representing concentrated loads was introduced by A. Mesnager, Comptes Rendus, vol. 164, 1917, p. 600, and has been used extensively by A. Nádai; see his book, Die elastischen Platten, 1925, p. 82.

$\Delta^2 z = 0$ (equation 16 with $w = 0$), at all points within the area, and in addition the following boundary conditions:

At the edges $x = 0$ and $x = s$ and at $y = \infty$:

$$z = \Delta z = 0 \qquad (28)$$

At $y = 0$:

$$\frac{\partial z}{\partial y} = 0 \text{ and } V_y = -\frac{1}{2}\,p = -\frac{P}{s}\sum_{1,2,\cdots}^{n}\sin\frac{n\pi u}{s}\sin\frac{n\pi x}{s} \qquad (29)$$

One may determine the function z by a partly deductive process. For the present purpose, it is sufficient however, to state the solution, and then verify it. The following solution [11] satisfies all the requirements:

$$z = \frac{Ps^2}{2\pi^3 N}\sum_{1,2\cdots}^{n}\frac{1}{n^3}\left(1 + \frac{n\pi y}{s}\right)e^{-\frac{n\pi y}{s}}\sin\frac{n\pi u}{s}\sin\frac{n\pi x}{s} \qquad (30)$$

It is seen immediately that $z = 0$ for $x = 0$ and $x = s$, and for $y = \infty$. One finds, furthermore,

$$\frac{\partial z}{\partial y} = -\frac{P}{2\pi N}\sum_{1,2,\cdots}^{n}\frac{1}{n}\,y e^{-\frac{n\pi y}{s}}\sin\frac{n\pi u}{s}\sin\frac{n\pi x}{s} \qquad (31)$$

which becomes zero when $y = 0$.

$$\frac{\partial^2 z}{\partial y^2} = -\frac{P}{2\pi N}\sum_{1,2,\cdots}^{n}\frac{1}{n}\left(1 - \frac{n\pi y}{s}\right)e^{-\frac{n\pi y}{s}}\sin\frac{n\pi u}{s}\sin\frac{n\pi x}{s} \qquad (32)$$

$$\frac{\partial^2 z}{\partial x^2} = -\frac{P}{2\pi N}\sum_{1,2,\cdots}^{n}\frac{1}{n}\left(1 + \frac{n\pi y}{s}\right)e^{-\frac{n\pi y}{s}}\sin\frac{n\pi u}{s}\sin\frac{n\pi x}{s} \qquad (33)$$

$$\Delta z = \frac{\partial^2 z}{\partial x^2} + \frac{\partial^2 z}{\partial y^2} = -\frac{P}{\pi N}\sum_{1,2,\cdots}^{n}\frac{1}{n}e^{-\frac{n\pi y}{s}}\sin\frac{n\pi u}{s}\sin\frac{n\pi x}{s} \qquad (34)$$

which becomes zero when $x = 0$, $x = s$, or $y = \infty$.

$$V_y = -N\frac{\partial \Delta z}{\partial y} = -\frac{P}{s}\sum_{1,2,\cdots}^{n}e^{-\frac{n\pi y}{s}}\sin\frac{n\pi u}{s}\sin\frac{n\pi x}{s} \qquad (35)$$

which assumes the required form when $y = 0$. Finally, one finds, $\frac{\partial^2 \Delta z}{\partial x^2} = -\frac{\partial^2 \Delta z}{\partial y^2}$, that is, $\Delta^2 z = 0$.

Nádai [12] observed (as may be verified without difficulty) that by introducing the function,

$$\varphi = N\Delta z = -\frac{P}{\pi}\sum_{1,2,\cdots}^{n}\frac{1}{n}e^{-\frac{n\pi y}{s}}\sin\frac{n\pi u}{s}\sin\frac{n\pi x}{s} \qquad (36)$$

one may restate equations 32 and 33 and express $\frac{\partial^2 z}{\partial x \partial y}$ in the following simple form:

$$2N\frac{\partial^2 z}{\partial x^2} = \varphi - y\frac{\partial \varphi}{\partial y} \qquad (37)$$

$$2N\frac{\partial^2 z}{\partial y^2} = \varphi + y\frac{\partial \varphi}{\partial y} \qquad (38)$$

$$2N\frac{\partial^2 z}{\partial x \partial y} = y\frac{\partial \varphi}{\partial x} \qquad (39)$$

Then one finds by equations 11, 12, and 13:

$$M_x = -\frac{1+\mu}{2}\varphi + \frac{1-\mu}{2}\,y\frac{\partial \varphi}{\partial y} \qquad (40)$$

$$M_y = -\frac{1+\mu}{2}\varphi - \frac{1-\mu}{2}\,y\frac{\partial \varphi}{\partial y} \qquad (41)$$

$$M_{xy} = -\frac{1-\mu}{2}\,y\frac{\partial \varphi}{\partial x} \qquad (42)$$

NÁDAI'S SOLUTION IN FINITE FORM PROVED

Nádai,[13] by a deductive process involving functions of a complex variable, derived an expression in finite form for the function φ in equations 36 to 42. Again, it will be sufficient here to state the expression and verify it.

The origin of coordinates is placed now at the center of the span, as in Figure 1. The edges have the equations $x = \pm\frac{s}{2}$, and the point of application of the load P has the coordinates $x = -v = -\frac{s}{2} + u$, $y = 0$. The expression found by Nádai, then, is stated as follows:

$$\varphi = N\Delta z = \frac{P}{4\pi}\log_e\frac{B}{A} \qquad (43)$$

where

$$A = \cosh\frac{\pi y}{s} + \cos\frac{\pi(x-v)}{s} \qquad (44)$$

$$B = \cosh\frac{\pi y}{s} - \cos\frac{\pi(x+v)}{s} \qquad (45)$$

The function φ in equation 43 is the same as the function φ in equation 36 (restated in terms of the new coordinates) if it satisfies the following requirements:

First, $\Delta\varphi = 0$ at all points except at the point of application of P.

Secondly, $\varphi = 0$ at $x = \pm\frac{s}{2}$ and for $y = \infty$.

Third, the total vertical shear at the circumference of a small circle drawn around the load shall be $-P$.

To show that the first requirement is satisfied, the derivatives of φ in equation 43 are expressed. One finds

$$\frac{\partial \varphi}{\partial x} = \frac{P}{4s}\left(\frac{\sin\frac{\pi(x+v)}{s}}{B} + \frac{\sin\frac{\pi(x-v)}{s}}{A}\right) \qquad (46)$$

$$\frac{\partial \varphi}{\partial y} = \frac{P}{4s}\sinh\frac{\pi y}{s}\left(\frac{1}{B} - \frac{1}{A}\right) \qquad (47)$$

Then, by use of the relation, $\cosh^2\frac{\pi y}{s} - \sinh^2\frac{\pi y}{s} = 1$, one finds

[11] A. Nádai, Die elastischen Platten, 1925, p. 85.
[12] A. Nádai, Die elastischen Platten, 1925, p. 86.
[13] A. Nádai, Die elastischen Platten, 1925, p. 89.

$$\left.\begin{array}{c}\dfrac{\partial^2\varphi}{\partial x^2}\\[4pt]-\dfrac{\partial^2\varphi}{\partial y^2}\end{array}\right\} = \frac{\pi P}{4s^2}\left[\frac{\cos\dfrac{\pi(x+v)}{s}\cosh\dfrac{\pi y}{s}-1}{B^2}+\right.$$

$$\left.\frac{\cos\dfrac{\pi(x-v)}{s}\cosh\dfrac{\pi y}{s}+1}{A^2}\right],$$

that is, $\Delta\varphi = \dfrac{\partial^2\varphi}{\partial x^2}+\dfrac{\partial^2\varphi}{\partial y^2}=0$.

The second requirement is satisfied because $A=B$ when $x=\pm\dfrac{s}{2}$, and because $\dfrac{B}{A}$ converges toward 1 when y increases indefinitely.

That the third requirement is satisfied, may be shown as follows: When α and β are small values, one may write, $\cos\alpha=1-\dfrac{\alpha^2}{2}$, $\cosh\beta=1+\dfrac{\beta^2}{2}$. Consequently, in the immediate neighborhood of the point $x=-v$, $y=0$, where $x+v$ and y are small, equation 45 may be replaced by the simpler expression,

$$B=\frac{\pi^2}{2s^2}(y^2+(x+v)^2)=\frac{\pi^2 r^2}{2s^2} \quad\text{------(48)}$$

Part III.—DERIVATION OF FORMULAS WHICH HAVE DIRECT APPLICATION TO THE PROBLEM OF BRIDGE FLOORS

DETERMINATION OF MOMENTS AT ONE POINT DUE TO A CONCENTRATED LOAD AT ANOTHER POINT

Using equations 40 to 47, one may express the bending moments M_x and M_y and the twisting moment M_{xy} produced at the point x, y by the load P at the point $-v$, 0. One finds

$$\left.\begin{array}{c}M_x\\ M_y\end{array}\right\}=\frac{(1+\mu)P}{8\pi}\log_e\frac{A}{B}\pm\frac{(1-\mu)Py}{8s}\sinh\frac{\pi y}{s}\left(\frac{1}{B}-\frac{1}{A}\right) \text{-(51)}$$

$$M_{xy}=-\frac{(1-\mu)Py}{8s}\left(\frac{\sin\dfrac{\pi(x-v)}{s}}{A}+\frac{\sin\dfrac{\pi(x+v)}{s}}{B}\right)\text{---(52)}$$

where

$$A=\cosh\frac{\pi y}{s}+\cos\frac{\pi(x-v)}{s},\ B=\cosh\frac{\pi y}{s}-\cos\frac{\pi(x+v)}{s}.$$

One may use these formulas to obtain expressions for the moments produced at the point $-v,0$ (the point of application of P_1 in Figure 1) by a load P at the point x, y. It is necessary for this purpose to let the points $-v$, 0 and x, y exchange significances. That is, one replaces x, y, and v by $-v$, $-y$, and $-x$, respectively. By this exchange the expressions for A and B remain the same. Denoting the new moments by M'_x, M'_y, and M'_{xy}, one finds

$$M'_x=M_x,\ M'_y=M_y \quad\text{------(53)}$$

$$M'_{xy}=\frac{(1-\mu)Py}{8s}\left(\frac{\sin\dfrac{\pi(x-v)}{s}}{A}-\frac{\sin\dfrac{\pi(x+v)}{s}}{B}\right)\text{-(54)}$$

That is, a law of reciprocity applies to the bending moments: The bending moments in the directions of x

where r is the distance between the points $-v$, 0 and x, y. Since $\log_e B$ is numerically large and varies rapidly in this neighborhood while $\log_e A$ varies relatively slowly, one may use for A the value at the point $x=-v$, $y=0$, that is,

$$A=1+\cos\frac{2\pi v}{s}=2\cos^2\frac{\pi v}{s} \quad\text{------(49)}$$

Then equation 43 assumes the following form, applicable when the distance r from the point of application of the load is small:

$$\varphi=\frac{P}{2\pi}\log_e\frac{\pi r}{2s\cos\dfrac{\pi v}{s}} \quad\text{------(50)}$$

Equations 17, for the vertical shears, may be written: $V_x=-\dfrac{\partial\varphi}{\partial x}\ V_y=-\dfrac{\partial\varphi}{\partial y}$. Correspondingly, the vertical shear in a section perpendicular to the radius vector r may be written: $V_r=-\dfrac{\partial\varphi}{\partial r}$. Then equation 50 gives $V_r=-\dfrac{P}{2\pi r}$, that is, the total shear at the circumference of the small circle with radius r is $-P$. Thus all the requirements are satisfied.

and y produced at point 1 by a load P at point 2 are the same as those produced at point 2 by a load P at point 1. It becomes unnecessary, therefore, to distinguish between M_x and M'_x, or between M_y and M'_y. The twisting moments, on the other hand, do not follow this law of reciprocity; M'_{xy} differs from M_{xy}.

With $\mu=0.15$, equations 51, 52, and 54 may be written as follows: [14]

$$\left.\begin{array}{c}M_x\\ M_y\end{array}\right\}=0.10536\ P\log_{10}\frac{A}{B}\pm$$

$$0.10625\frac{Py}{s}\sinh\frac{\pi y}{s}\left(\frac{1}{B}-\frac{1}{A}\right)\text{--------(55)}$$

$$\left.\begin{array}{c}M_{xy}\\ M'_{xy}\end{array}\right\}=-0.10625\frac{Py}{s}\left(\frac{\sin\dfrac{\pi(x+v)}{s}}{B}\pm\frac{\sin\dfrac{\pi(x-v)}{s}}{A}\right)\text{-(56)}$$

EFFECTS OF LOAD DISTRIBUTED UNIFORMLY OVER THE AREA OF A SMALL CIRCLE

Consider now a load P which is distributed uniformly over the area of a small circle with center at the point $-v$, 0 and with the diameter c, as P_1 in Figure 1. In order to obtain the correct maximum tensile stress at the bottom of the slab by use of the ordinary theory of flexure, the moments will be determined (as proposed in the introduction) as if the load were distributed uniformly over the area of a circle with diameter c_1 instead of c.[15]

By using polar coordinates r, θ, with the pole at the center of the circle, and with the angle θ measured from the x-axis, the load on an element of the area of the

---

[14] Numerical computations based on these equations are made conveniently by use of the tables published by K. Hayashi, Sieben- und mehrstellige Tafeln der Kreis- und Hyperbelfunktionen und deren Produkte sowie der Gammafunktion. (Berlin), 1926.
[15] See footnote 3 on p. 2 and the explanation following this reference.

circle will be expressed as $\frac{4P}{\pi c_1^2}\,r\,dr\,d\theta$. On account of the reciprocal relation of bending moments (equations 53), the bending moments produced at the center of the circle may be computed by means of equation 51. Since the distances are small, the values of A and B may be taken from equations 49 and 48, respectively. The term $\frac{1}{A}$ at the end of equation 51 may be ignored as insignificant in comparison with $\frac{1}{B}$. Moreover, $\sinh\frac{\pi y}{s}$ may be replaced by $\frac{\pi y}{s}$. Then equation 51 leads to the following values of the resultant moments at the center of the circle:

$$\left.\begin{array}{c}M_x\\M_y\end{array}\right\} = \int_{-\pi}^{\pi}d\theta\int_0^{\frac{c_1}{2}}\frac{4P}{\pi c_1^2}r\,dr\left(\frac{1+\mu}{4\pi}\log_e\frac{2s\cos\frac{\pi v}{8}}{\pi r}\pm\frac{(1-\mu)\sin^2\theta}{4\pi}\right).$$

Since $\int_0^{\frac{c_1}{2}}r\,dr\,\log_e r = \frac{c_1^2}{8}\left(\log_e\frac{c_1}{2}-\frac{1}{2}\right)$, one finds

$$\left.\begin{array}{c}M_x\\M_y\end{array}\right\} = \frac{(1+\mu)P}{4\pi}\left(\log_e\left(\frac{4s}{\pi c_1}\cos\frac{\pi v}{8}\right)+\frac{1}{2}\right)\pm\frac{(1-\mu)}{8\pi}P \quad\quad(57)$$

The equivalent diameter c_1 is expressed with satisfactory approximation by the following formula,[16] applicable when $c<3.45h$:

$$c_1 = 2(\sqrt{0.4c^2+h^2}-0.675\,h) \quad\quad\quad (58)$$

GREATEST BENDING MOMENTS COMPUTED FOR CASE OF WHEEL LOAD AT CENTER

When the load is at the center, that is, $v=0$, the moments M_x and M_y in equation 57 assume the following values, which are denoted by M_{0x} and M_{0y}, respectively:

$$M_{0x} = \frac{P}{4\pi}\left((1+\mu)\log_e\frac{4s}{\pi c_1}+1\right) \quad\quad (59)$$

$$M_{0y} = M_{0x}-\frac{(1-\mu)P}{4\pi} \quad\quad\quad (60)$$

or, with $\mu=0.15$, and c_1 substituted from equation 58:

$$M_{0x}=0.21072\,P\left[\log_{10}\frac{8}{h}-\log_{10}\left(\sqrt{0.4\frac{c^2}{h^2}+1}-0.675\right)+0.1815\right] \quad\quad (61)$$

$$M_{0y}=M_{0x}-0.0676\;P \quad\quad\quad (62)$$

---

[16] Equation 8 in the paper by the writer, Stresses in Concrete Pavements Computed by Theoretical Analysis, Public Roads, vol. 7, No. 2, April, 1926.
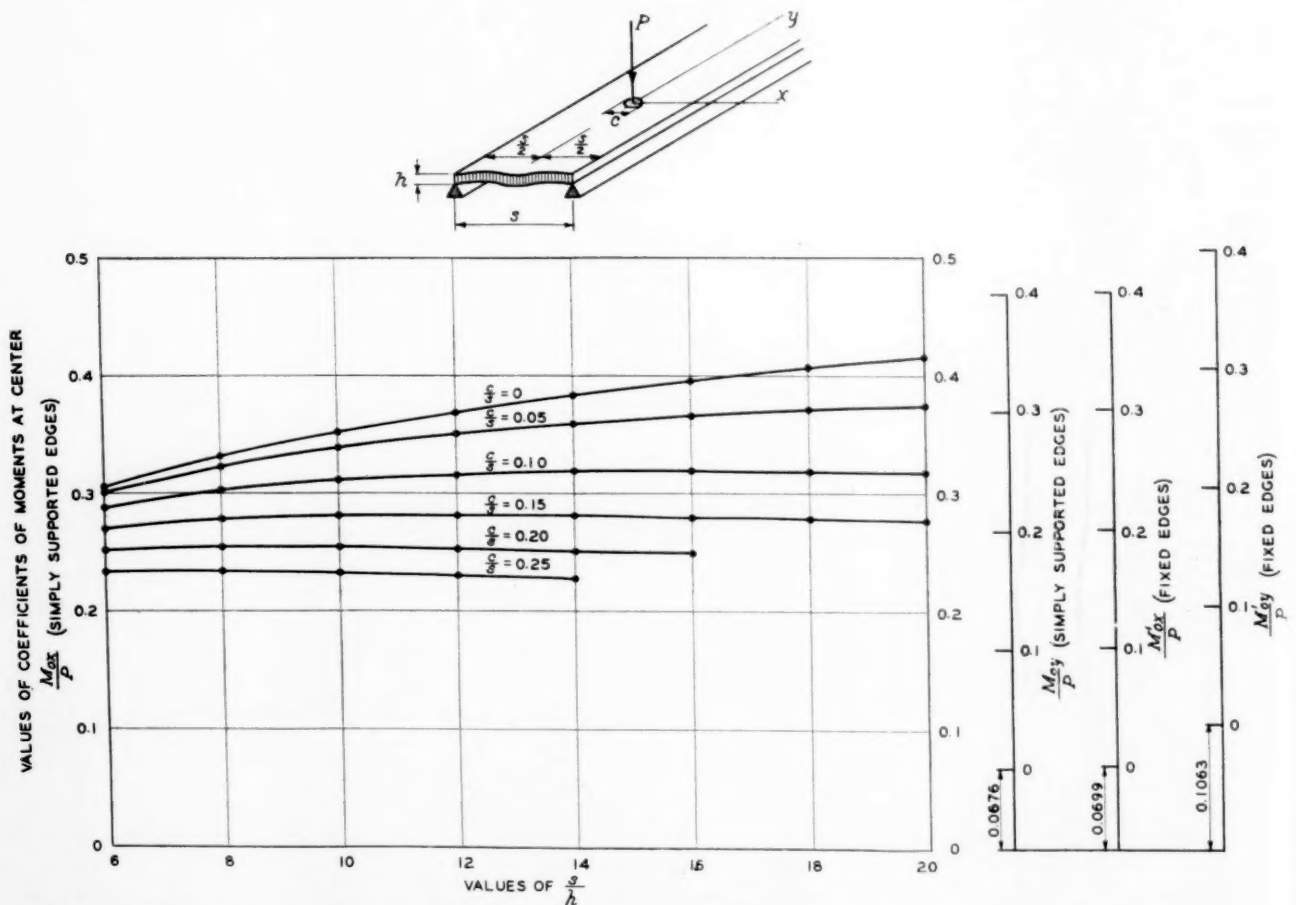

FIGURE 6.—COEFFICIENTS OF BENDING MOMENTS, M_{0x} AND M_{0y}, IN DIRECTIONS OF x AND y, RESPECTIVELY, PRODUCED AT CENTER OF SLAB BY A CENTRAL LOAD P DISTRIBUTED UNIFORMLY OVER THE AREA OF A SMALL CIRCLE WITH DIAMETER c. RESULTS REPRESENTING EQUATIONS 61, 62, 104, AND 105. NUMERICAL VALUES STATED IN TABLE 1. POISSON'S RATIO, $\mu=0.15$

TABLE 1.—*Values of the coefficient $\frac{M_{0x}}{P}$ of the maximum bending moment per unit of width, produced at the center of the slab in the direction of the span by a central load P distributed uniformly over the area of a small circle with diameter c. The edges are assumed to be simply supported. The values were computed from equation 61 for different relative values of the span, s, the thickness, h, and the diameter c. Figure 6 shows the results graphically. Poisson's ratio, $\mu = 0.15$*

	$c=0$	$c=0.05s$	$c=0.10s$	$c=0.15s$	$c=0.20s$	$c=0.25s$
$s=6h$	0.3051	0.3003	0.2874	0.2701	0.2520	0.2345
$s=8h$	.3315	.3230	.3026	.2784	.2552	.2345
$s=10h$	.3519	.3390	.3110	.2811	.2550	.2326
$s=12h$	.3685	.3508	.3154	.2815	.2535	.2303
$s=14h$	.3827	.3595	.3178	.2809	.2516	.2284
$s=16h$	.3949	.3660	.3186	.2798	.2499	....
$s=18h$	.4056	.3709	.3186	.2786	....	....
$s=20h$	.4153	.3744	.3184	.2771	....	....

Table 1 and Figure 6 show values of the coefficient $\frac{M_{0x}}{P}$ computed from equation 61. The coefficients stated are pure numbers. If, for example, one reads in Figure 6, $\frac{M_{0x}}{P} = 0.3$, the significance is: $M_{0x} = 0.3 P$, or, with $P = 10,000$ pounds, $M_{0x} = 0.3 \times 10,000$ pounds $= 3,000$ pounds $= 3,000 \frac{\text{in. lbs.}}{\text{in.}} = 3,000 \frac{\text{ft. lbs.}}{\text{ft.}}$ (the unit of bending moment per unit of width being inch-pounds per inch or foot-pounds per foot or simply pounds). If units of the metric system were used, the coefficients in Figure 6 would remain unchanged. These comments apply also to the coefficients stated in the diagrams and tables which are given later.

Since the difference between $\frac{M_{0x}}{P}$ and $\frac{M_{0y}}{P}$ is constant, the curves in Figure 6 also represent values of $\frac{M_{0y}}{P}$, on a separate scale. The third scale from the right serves this purpose.

The moment M_{0x} could be produced as the maximum moment per unit of width in a simple beam with span s and width b_e, the load P being applied at the center of the span, and distributed over the width of the beam. Ignoring the effects of Poisson's ratio, one may assume the bending moment to be distributed uniformly over the width. The width b_e bringing about this equivalence of a slab and a beam is called the effective width.[17] It is defined by the equation,

$$M_{0x} = \frac{1}{4} \frac{P}{b_e} s \quad\text{------------} (63)$$

or,

$$b_e = \frac{Ps}{4 M_{0x}} \quad\text{------------} (64)$$

Values of b_e, computed from this equation, with M_{0x} defined by equation 61, are shown in Table 2 and Figure 7. Knowing b_e one may compute the bending moments by equation 63.

The diagram at the right of Figure 7 shows a set of straight horizontal lines which may be allowed to take the place of the curves in a crude, approximate computation. To be on the side of safety the straight lines should be drawn so as to represent the low values rather than the average values defined by the curves. The straight lines are drawn according to the formula,

$$b_e = 0.58s + 2c \quad\text{------------} (65)$$

[17] E. F. Kelley, Effective Width of Concrete Bridge Slabs Supporting Concentrated Loads, Public Roads, vol. 7, No. 1, March, 1926, p. 7.
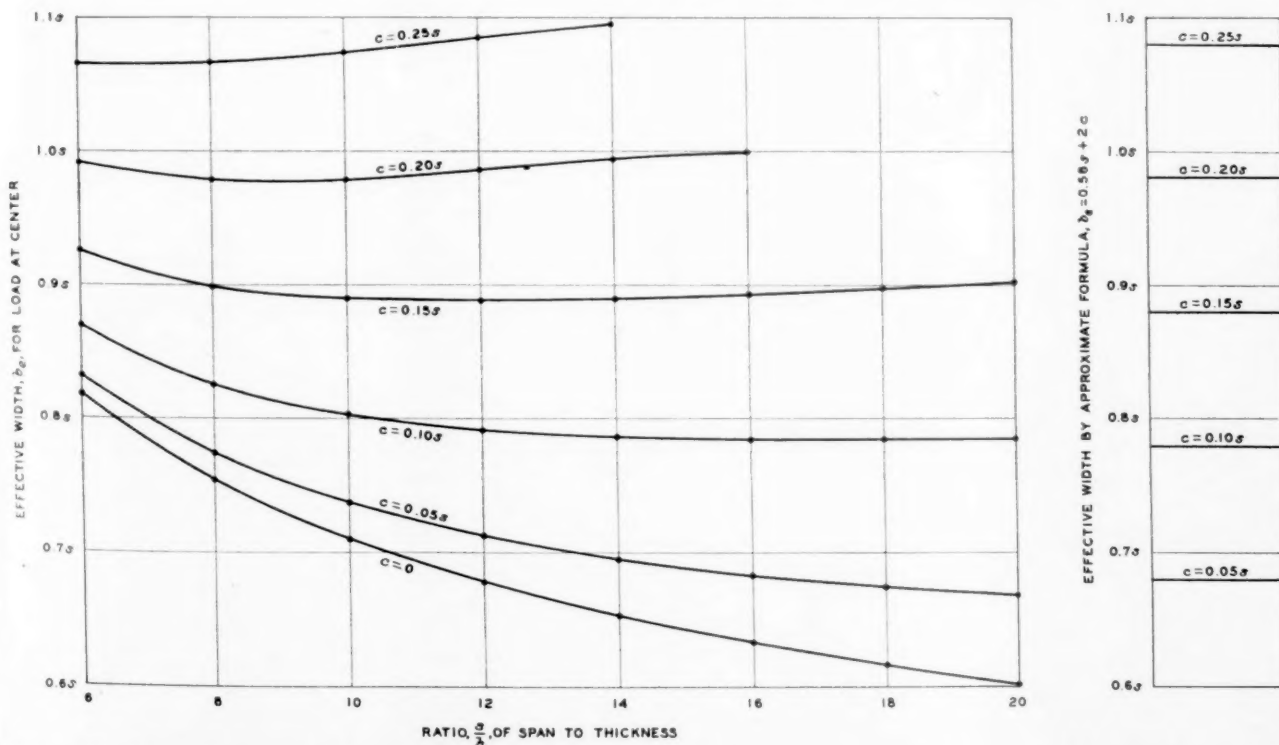

FIGURE 7.—EFFECTIVE WIDTH b_e FOR CENTRAL LOAD, DISTRIBUTED UNIFORMLY OVER THE AREA OF A SMALL CIRCLE WITH DIAMETER c, WHEN THE EDGES ARE SIMPLY SUPPORTED (FROM EQUATIONS 64 AND 65, AND TABLE 2). POISSON'S RATIO, $\mu = 0.15$

98022—30——2

A corresponding, roughly approximate expression for the bending moment is obtained by substituting this value of b_e in equation 63:

$$M_{0x} = \frac{Ps}{2.32s + 8c} \quad \text{-------------(66)}$$

TABLE 2.—*Values of the ratio,* $\frac{b_e}{s}$, *of the effective width to the span, in the cases represented in Table 1. The values were computed from equations 64 and 61, and are represented graphically in Figure 7. Poisson's ratio,* $\mu=0.15$

	$c=0$	$c=0.05s$	$c=0.10s$	$c=0.15s$	$c=0.20s$	$c=0.25s$
$s=6h$	0.819	0.832	0.870	0.925	0.992	1.066
$s=8h$	.754	.774	.826	.808	.980	1.066
$s=10h$	.710	.737	.804	.890	.980	1.075
$s=12h$	.678	.713	.792	.888	.986	1.085
$s=14h$	.653	.695	.787	.890	.994	1.095
$s=16h$	.633	.683	.785	.893	1.000	----------
$s=18h$	.616	.674	.785	.897	----------	----------
$s=20h$	.602	.668	.785	.902	----------	----------

MOMENTS COMPUTED FOR CASE OF TWO WHEEL LOADS ON LINE IN DIRECTION OF SPAN

Figure 8 (a) shows the case of two wheel loads, P_1 at he point 0, 0, and P_2 at the point x, 0. The effects produced by P_1 at the point of application of P_1 are expressed by equations 59 and 61, and are represented in Table 1 and Figure 6. The moments contributed at the point of application of P_1 in Figure 8 (a) by P_2 may be obtained from equation 51. One finds

$$\frac{A}{B} = \frac{1+\cos\frac{\pi x}{s}}{1-\cos\frac{\pi x}{s}} = \cot^2\frac{\pi x}{2s},$$

and consequently,
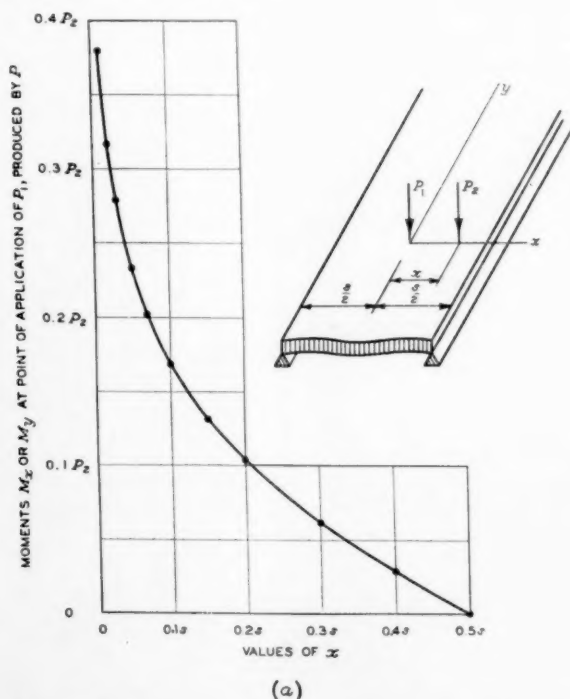
$$M_x = M_y = \frac{(1+\mu)P_2}{4\pi} \log_e \cot \frac{\pi x}{2s} \quad \text{-------(67)}$$

or, with $\mu=0.15$,

$$M_x = M_y = 0.21072\, P_2 \log_{10} \cot \frac{\pi x}{2s} \quad \text{------(68)}$$

Table 3 and the curve in Figure 8 (a) represent values computed from equation 68.

TABLE 3.—*Coefficients* $\frac{M_x}{P_2}$ *and* $\frac{M_y}{P_2}$ *of the moments produced at the point 0, 0 by the load P_2 at the point x, 0, computed from equation 68, and represented graphically in Figure 8 (a). Poisson's ratio,* $\mu=0.15$

$\frac{x}{s}$	$\frac{M_x}{P_2} = \frac{M_y}{P_2}$	$\frac{x}{s}$	$\frac{M_x}{P_2} = \frac{M_y}{P_2}$
0.01	0.3801	0.15	0.1306
.02	.3166	.20	.1029
.03	.2795	.30	.0617
.05	.2326	.40	.0292
.07	.2017	.50	0
.10	.1686		

When there is a fixed distance a between the two loads, the moments under P_1 may be increased by moving the loads toward the left, into the positions of P_1 and P_2 in Figure 1. With P_1 and P_2 at the points $-v$, 0 and $a-v$, 0, respectively, and $P_1=P_2=P$, the moments under P_1 may be expressed as follows, by use of equations 57, 59, 51, and 60:

$$M_x = M_{0x} + \frac{(1+\mu)P}{4\pi} \log_e \cos \frac{\pi v}{s} +$$

$$\frac{(1+\mu)P}{8\pi} \log_e \frac{1+\cos\frac{\pi(a-2v)}{s}}{1-\cos\frac{\pi a}{s}} \quad \text{------(69)}$$
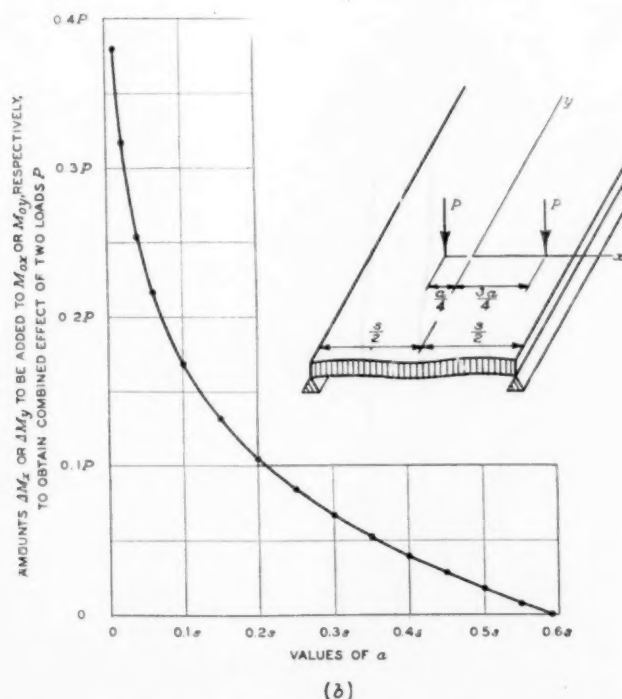
(a)

(b)

FIGURE 8.—BENDING MOMENTS PRODUCED AT POINT OF APPLICATION OF LEFT OF TWO LOADS (FROM EQUATIONS 68 AND 72, AND TABLES 3 AND 4). POISSON'S RATIO, $\mu=0.15$

$$M_y = M_x - \frac{(1-\mu)P}{4\pi} \quad \text{------------} \quad (70)$$

Since $1 + \cos\frac{\pi(a-2v)}{s} = 2\cos^2\frac{\pi(a-2v)}{2s}$, these moments reach their maximum values when the product $f = \cos\frac{\pi v}{s}\cos\frac{\pi(a-2v)}{2s}$, becomes a maximum. By writing $f = \frac{1}{2}\left(\cos\frac{\pi(a-4v)}{2s} + \cos\frac{\pi a}{2s}\right)$, one finds that the condition, $\frac{df}{dv} = 0$, gives $\sin\frac{\pi(a-4v)}{2s} = 0$, or $v = \frac{a}{4}$. That is, the two equal loads are placed as they would be on a beam. With $v = \frac{a}{4}$, equation 69 becomes,

$$M_x = M_{0x} + \frac{(1+\mu)P}{4\pi}\log_e \frac{\cot\frac{\pi a}{4s}}{2} \quad \text{------} \quad (71)$$

or, with $\mu = 0.15$,

$$\left.\begin{array}{l} \dfrac{\Delta M_x}{P} = \dfrac{M_x - M_{0x}}{P} \\[2mm] \dfrac{\Delta M_y}{P} = \dfrac{M_y - M_{0y}}{P} \end{array}\right\} = 0.21072\log_{10}\frac{\cot\frac{\pi a}{4s}}{2} \quad \text{---} \quad (72)$$

These values become negative when $a > 0.5903s$. In this case the greatest effect is produced by P_1 alone, placed at the center of the span.

Table 4 and Figure 8 (b) show values computed from equation 72.

TABLE 4.—*Values* $\frac{\triangle M_x}{P}$ *or* $\frac{\triangle M_y}{P}$ *to be added to* $\frac{M_{0x}}{P}$ *(given in Table 1) or* $\frac{M_{0y}}{P}$ *(equation 62), respectively, to obtain the values of* $\frac{M_x}{P}$ *or* $\frac{M_y}{P}$ *due to the combined action of two loads P placed at the points* $-\frac{a}{4}, 0$ *and* $\frac{3a}{4}, 0$, *computed from equation 72, and represented graphically in Figure 8 (b). Poisson's ratio, $\mu=0.15$*

$\frac{a}{s}$	$\frac{\Delta M_x}{P} = \frac{\Delta M_y}{P}$	$\frac{a}{s}$	$\frac{\Delta M_x}{P} = \frac{\Delta M_y}{P}$
0.01	0.3801	0.30	0.0671
.02	.3167	.35	.0524
.04	.2532	.40	.0394
.06	.2161	.45	.0278
.10	.1692	.50	.0172
.15	.1319	.55	.0074
.20	.1052	.5903	0
.25	.0844		

MOMENTS COMPUTED FOR TWO LOADS ON CENTER LINE

Figure 9 shows two loads, P_1 at the point 0, 0, and P_3 at the point 0, y. The moments produced under P_1 by P_1 are given by equations 59 to 62 and in Table 1 and Figure 6. To these moments must be added the moments M_x and M_y contributed at the point of application of P_1 by P_3. Equation 51, with $x = v = 0$, that is, with

$$A = \cosh\frac{\pi y}{s} + 1 = 2\cosh^2\frac{\pi y}{2s},$$

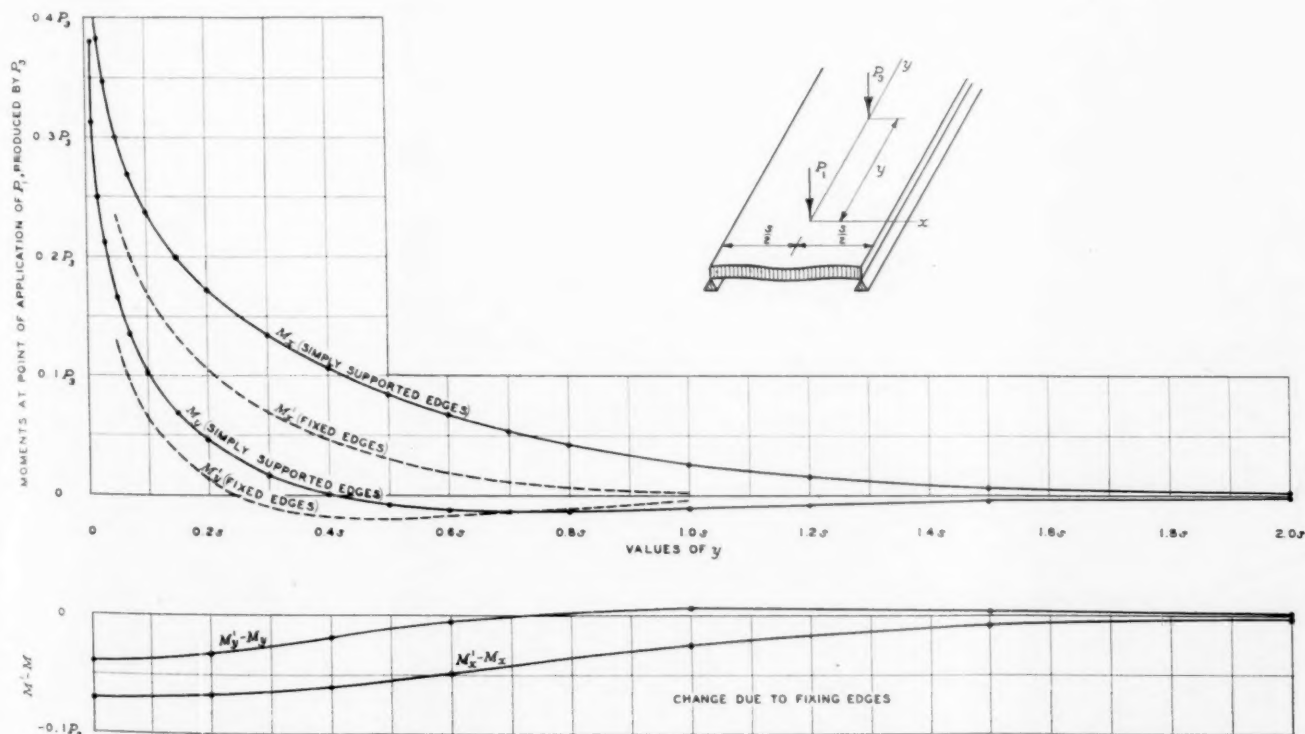$$B = \cosh\frac{\pi y}{s} - 1 = 2\sinh^2\frac{\pi y}{2s},$$

FIGURE 9.—BENDING MOMENTS PRODUCED AT POINT OF APPLICATION OF P_1 BY P_3 (FROM EQUATIONS 74, 102, AND 103, AND TABLES 5 AND 7). POISSON'S RATIO, $\mu=0.15$

and with $P=P_3$, gives

$$\left.\begin{array}{c}M_x\\M_y\end{array}\right\}=\frac{(1+\mu)P_3}{4\pi}\log_e\coth\frac{\pi y}{2s}\pm\frac{(1-\mu)P_3 y}{4s\sinh\frac{\pi y}{s}} \text{ ---- (73)}$$

or, with $\mu=0.15$,

$$\left.\begin{array}{c}M_x\\M_y\end{array}\right\}=0.21072P_3\log_{10}\coth\frac{\pi y}{2s}\pm\frac{0.2125P_3 y}{s\sinh\frac{\pi y}{s}} \text{ --- (74)}$$

Coefficients $\dfrac{M_x}{P_3}$ and $\dfrac{M_y}{P_3}$, computed from equation 74, are stated in the first section of Table 5. Equation 74 is represented graphically by the curves drawn with full lines in the upper part of Figure 9.

MOMENTS COMPUTED AT CENTER FOR LOAD AT ANY POINT, AND ALSO AT ANY POINT FOR LOAD AT CENTER

Table 5 and Figures 8 to 14 show moments produced at points x, y by a load, $P=1$, at the center, point 0, 0, and moments produced at point 0, 0 by a load, $P=1$,

at points x, y, for Poisson's ratio, $\mu=0.15$. All of these moments are defined by equations 44, 45, 55, 56, with $v=0$. Equations 68 and 74 apply to the special cases of $y=0$ and $x=0$, respectively. With $v=0$, the equations for the twisting moments (equations 52 and 54, or equation 56 when $\mu=0.15$) may be written in the simpler forms,

$$M_{xy}=-\frac{(1-\mu)Py}{2s}\frac{\sin\frac{\pi x}{s}\cosh\frac{\pi y}{s}}{\cosh\frac{2\pi y}{s}-\cos\frac{2\pi x}{s}} \text{ ---- (75)}$$

$$M'_{xy}=-\frac{(1-\mu)\ Py}{4s}\frac{\sin\frac{2\pi x}{s}}{\cosh\frac{2\pi y}{s}-\cos\frac{2\pi x}{s}} \text{ --- (76)}$$

In the special case, $x=\dfrac{s}{2}$, that is, at the edge, these equations give

FIGURE 10.—BENDING MOMENTS M_x, PRODUCED AT POINT x, y BY LOAD $P=1$ AT 0, OR AT 0 BY LOAD $P=1$ AT POINT x, y (FROM EQUATION 55 AND TABLE 5). POISSON'S RATIO, $\mu=0.15$
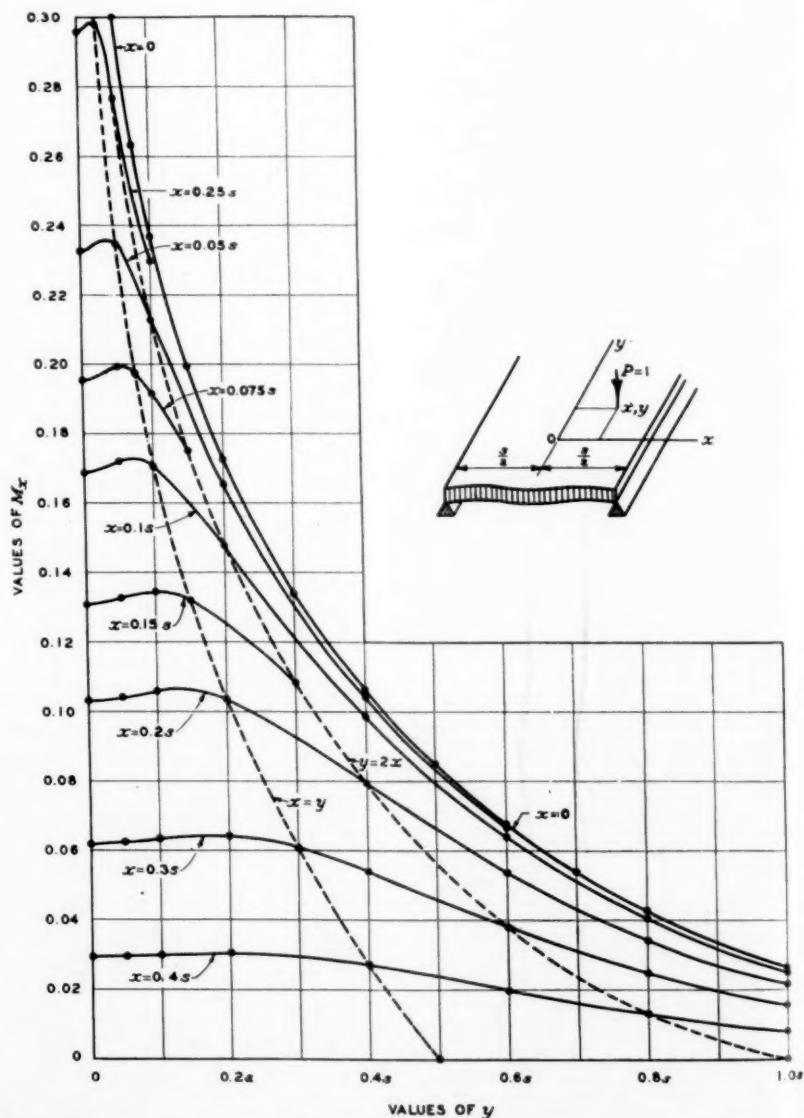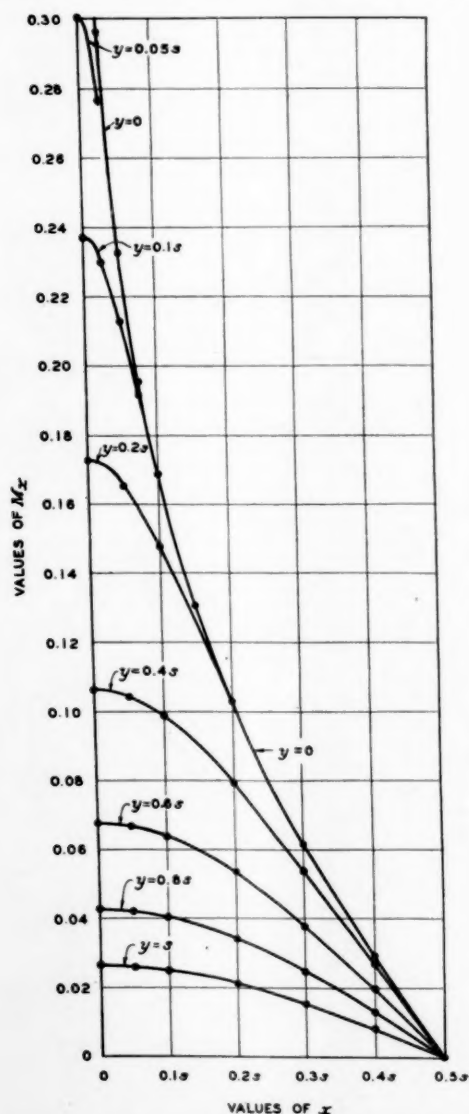
FIGURE 11.—BENDING MOMENTS M_y, PRODUCED AT POINT x, y BY LOAD $P=1$ AT 0, OR AT 0 BY LOAD $P=1$ AT POINT x, y (FROM EQUATION 55 AND TABLE 5). POISSON'S RATIO, $\mu=0.15$
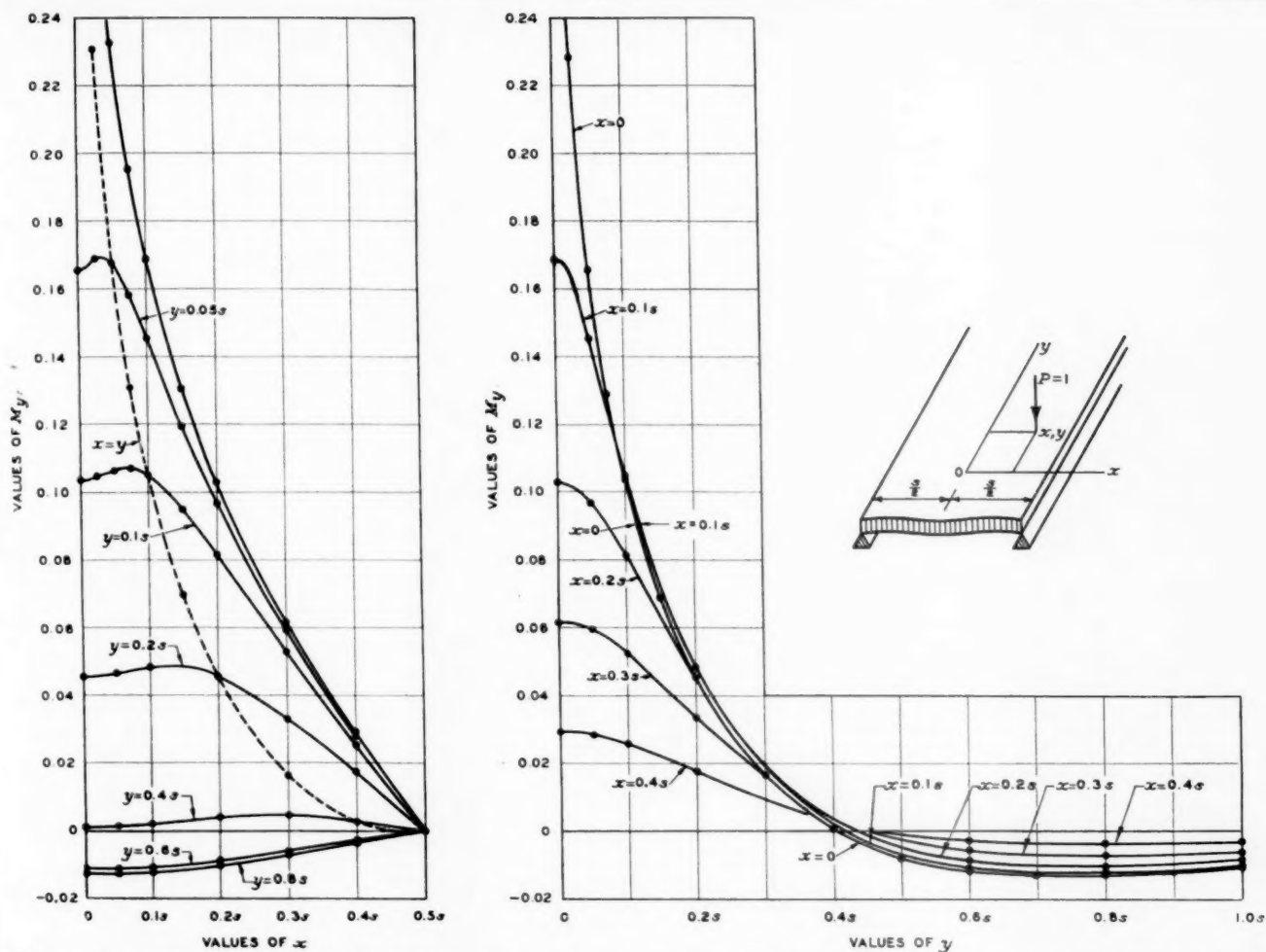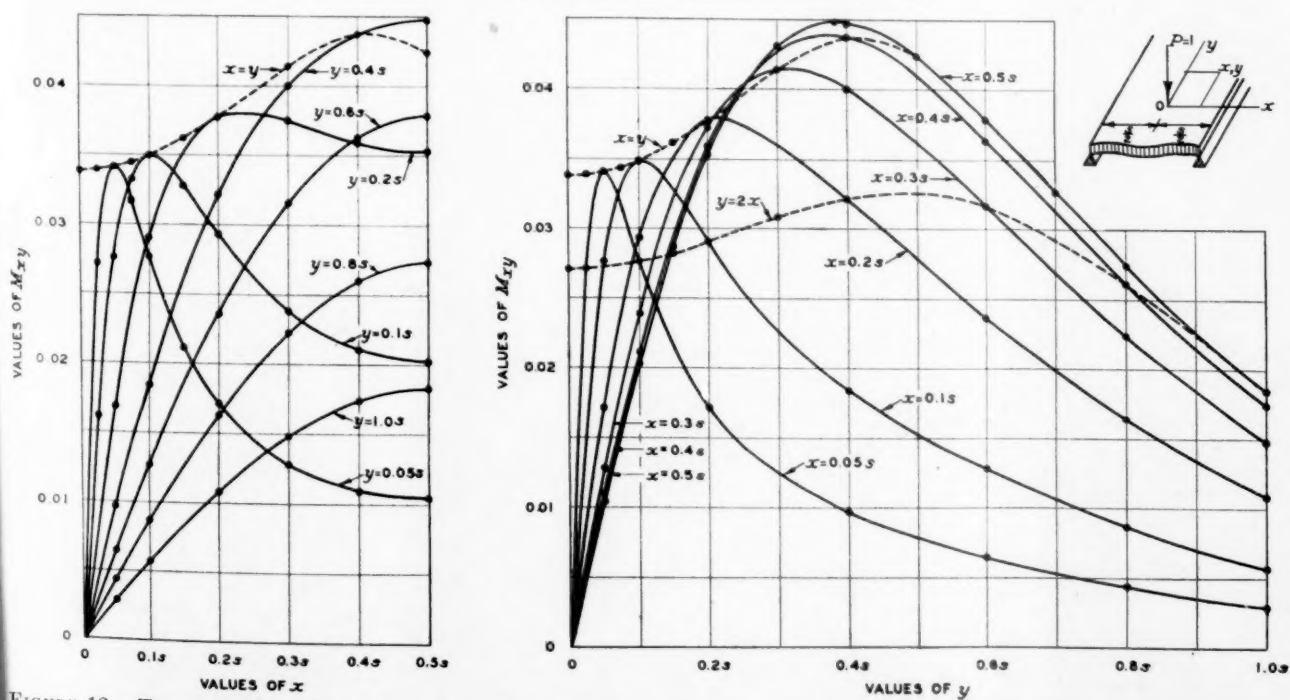

FIGURE 12.—TWISTING MOMENTS M_{xy}, PRODUCED AT POINT x, y BY LOAD $P=1$ AT 0 (FROM EQUATIONS 56, 75, AND 77, AND TABLE 5). POISSON'S RATIO, $\mu=0.15$
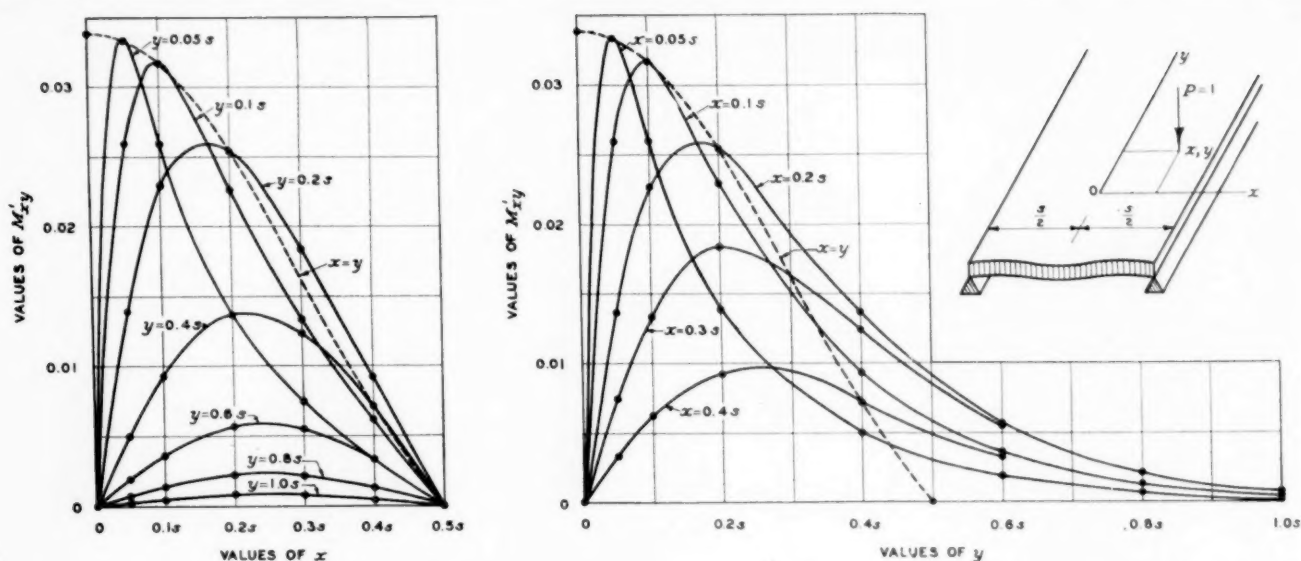
FIGURE 13.—TWISTING MOMENTS M'_{xy}, PRODUCED AT 0 BY LOAD $P=1$ AT POINT x, y (FROM EQUATIONS 56 AND 76, AND TABLE 5). POISSON'S RATIO, $\mu=0.15$

TABLE 5.—*Bending moments M_x and M_y produced at point x, y by load $P=1$, at point 0, 0, or at point 0, 0 by load $P=1$ at point x, y, computed from equations 44, 45, 55 (with $v=0$), 68 and 74, and represented graphically in Figures 8 (a), 9, 10, 11, and 14. Twisting moments M_{xy} produced at point x, y by load $P=1$ at point 0, 0, and twisting moments M'_{xy} produced at point 0, 0 by load $P=1$ at point x, y, computed from equations 44, 45, 56 (with $v=0$), 75, 76, and 77, and represented graphically in Figures 12, 13, and 14. Poisson's ratio, $\mu=0.15$*

$\frac{x}{s}$	$\frac{y}{s}$	M_x	M_y	$-M_{xy}$	$-M'_{xy}$
0	0.01	0.448	0.313	0	0
	.02	.384	.249	0	0
	.025	.3639	.2287	0	0
	.03	.347	.212	0	0
	.05	.3004	.1657	0	0
	.07	.269	.135	0	0
	.075	.2632	.1291	0	0
	.1	.2367	.1036	0	0
	.15	.1992	.0688	0	0
	.2	.1723	.0455	0	0
	.3	.1339	.0167	0	0
	.4	.1062	.0009	0	0
	.5	.0848	−.0076	0	0
	.6	.0676	−.0116	0	0
	.7	.0538	−.0130	0	0
	.8	.0426	−.0129	0	0
	1.0	.0263	−.0105	0	0
	1.2	.0160	−.0076	0	0
	1.5	.0074	−.0041	0	0
	2.0	.0019	−.0013	0	0
	2.5	.0005	−.0003	0	0
	3.0	.0001	−.0001	0	0
.01	0	.3801	.3801	0	0
.02	0	.3166	.3166	0	0
.025	0	.2962	.2962	0	0
	.025	.2983	.2308	.03389	
	.05	.2766	.1689	.02719	
	.1	.2299	.1048	.01619	
.03	0	.2795	.2795	0	0
.05	0	.2326	.2326	0	0
	.05	.2346	.1676	.03410	.03327
	.1	.2128	.1067	.02760	.02596
	.2	.1653	.0466	.01689	.01385
	.4	.1043	.0012	.00959	.00499
	.6	.0667	−.0114	.00648	.00190
	.8	.0420	−.0127	.00439	.00069
	1.0	.0260	−.0104	.00289	.00025
.07	0	.2017	.2017	0	0
.075	0	.1953	.1953	0	0
	.05	.1992	.1581	.03164	
	.075	.1972	.1308	.03444	
	.1	.1915	.1071	.03328	
	.15	.1750	.0717	.02822	
.1	0	.1686	.1686	0	0
	.05	.1719	.1454	.02761	.02594
	.1	.1704	.1050	.03491	.03163
	.2	.1478	.0483	.02902	.02292

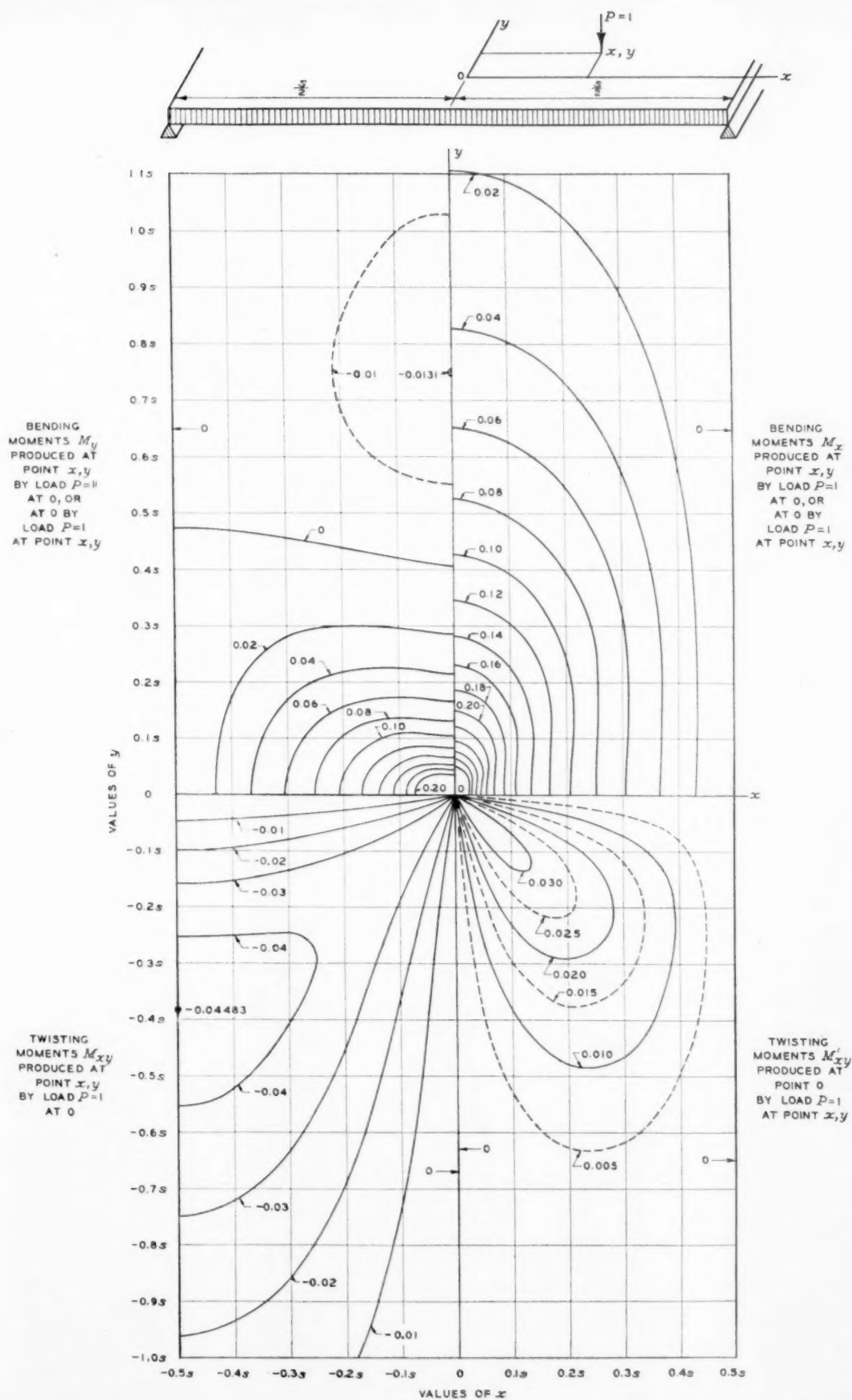| $\frac{x}{s}$	$\frac{y}{s}$	M_x	M_y	$-M_{xy}$	$-M'_{xy}$
0.1	0.4	0.0987	0.0021	0.01846	0.00925
	.6	.0639	−.0108	.01271	.00359
	.8	.0404	−.0122	.00866	.00132
	1.0	.0250	−.0100	.00571	.00047
.15	0	.1306	.1306	0	0
	.05	.1324	.1195	.02114	
	.1	.1342	.0949	.03287	
	.15	.1319	.0695	.03619	
	.3	.1083	.0194	.03076	
.2	0	.1029	.1029	0	0
	.05	.1040	.0967	.01707	.01364
	.1	.1058	.0813	.02930	.02258
	.2	.1035	.0455	.03783	.02542
	.4	.0793	−.0040	.03214	.01369
	.6	.0535	−.0086	.02361	.00567
	.8	.0342	−.0102	.01636	.00214
	1.0	.0213	−.0084	.01083	.00075
.3	0	.0617	.0617	0	0
	.05	.0622	.0593	.01281	.00744
	.1	.0632	.0526	.02386	.01336
	.2	.0640	.0337	.03749	.01831
	.3	.0607	.0164	.04145	
	.4	.0540	.0046	.04005	.01239
	.6	.0380	−.0058	.03157	.00551
	.8	.0247	−.0073	.02233	.00211
	1.0	.0154	−.0061	.01487	.00075
.4	0	.0292	.0292	0	0
	.05	.0294	.0283	.01401	.00336
	.1	.0298	.0257	.02108	.00621
	.2	.0305	.0175	.03594	.00922
	.4	.0271	.0029	.04373	.00711
	.6	.0197	−.0029	.03629	.00333
	.8	.0129	−.0038	.02608	.00130
	1.0	.0081	−.0032	.01745	.00047
.5	0	0	0	0	0
	.05	0	0	.01049	0
	.1	0	0	.02024	0
	.15	0	0	.02864	0
	.2	0	0	.03530	0
	.3	0	0	.04313	0
	.382	0	0	.04483	0
	.4	0	0	.04476	0
	.5	0	0	.04234	0
	.6	0	0	.03785	0
	.7	0	0	.03259	0
	.8	0	0	.02736	0
	.0	0	0	.01833	0
	11.2	0	0	.01175	0
	1.5	0	0	.00573	0
	2.0	0	0	.00159	0

FIGURE 14.—CONTOUR LINES OF SURFACES REPRESENTING MOMENTS (COMPARE FIGURES 10 TO 13).
POISSON'S RATIO, $\mu = 0.15$

$$M_{xy} = - \frac{(1-\mu)\ Py}{4s \cosh \frac{\pi y}{s}} \quad\text{---------} (77)$$

and $M'_{xy} = 0$.

For small values of x and y, that is, in the immediate neighborhood of the point 0, 0, one may write

$$\sin \frac{2\pi x}{s} = 2 \sin \frac{\pi x}{s} = \frac{2\pi x}{s}, \cosh \frac{\pi y}{s} = 1, \text{ and}$$

$$\cosh \frac{2\pi y}{s} - \cos \frac{2\pi x}{s} = \frac{2\pi^2}{s^2}(y^2 + x^2).$$

Then equations 75 and 76 may be written

$$M_{xy} = M'_{xy} = - \frac{(1-\mu)\ P}{4\pi}\ \frac{xy}{x^2+y^2} = - \frac{(1-\mu)\ P}{8\pi} \sin 2\theta \quad (78)$$

where θ is the angle between the x-axis and the radius vector to the point x, y; or, with $\mu = 0.15$,

$$M_{xy} = M'_{xy} = -0.06764\ P\ \frac{xy}{x^2+y^2}$$
$$= -0.03382\ P \sin 2\theta \quad\text{-----------} (79)$$

With $x = y$, equation 79 gives $M_{xy} = M'_{xy} = -0.03382P$. With $x = 2y$ or $y = 2x$, the same equation gives $M_{xy} = M'_{xy} = -0.02706P$.

Attention is called especially to Figure 14, showing contour lines of the surfaces representing the moments.

COMPUTATION OF MOMENTS PRODUCED AT POINT OF APPLICATION OF P_1 IN FIGURE 1 BY THE TWO LOADS P_3 AND P_4

The two loads P_3 and P_4 in Figure 1 will be assumed to be equal, each equal to P. In order to determine the value of v at which the bending moments produced at the point $-v$, 0 by the two loads become as large as possible, the following conditions are introduced temporarily: $P = 1$, $s = \pi$, y-axis at the left edge. Then equations 32 and 33 lead to an expression of the following form for the bending moment M_x produced at point u, 0 by the load $P = 1$ at the point x, b:

$$M = \sum_{1,2,\cdots}^{n} C_n \sin nu \sin nx \quad\text{----------} (80)$$

where the coefficients C_n are functions of b only. The same formula, only with different values of C_n, expresses the corresponding value of M_y. The two loads $P = 1$ at the points u, b and $u + a$, b then produce the moment,

$$M = \sum_{1,2,\cdots}^{n} C_n \sin nu\ (\sin nu + \sin n(u+a))$$

$$= \sum_{1,2,\cdots}^{n} \frac{C_n}{2}(1 - \cos 2\ nu + \cos na - \cos n(2u+a)) \quad (81)$$
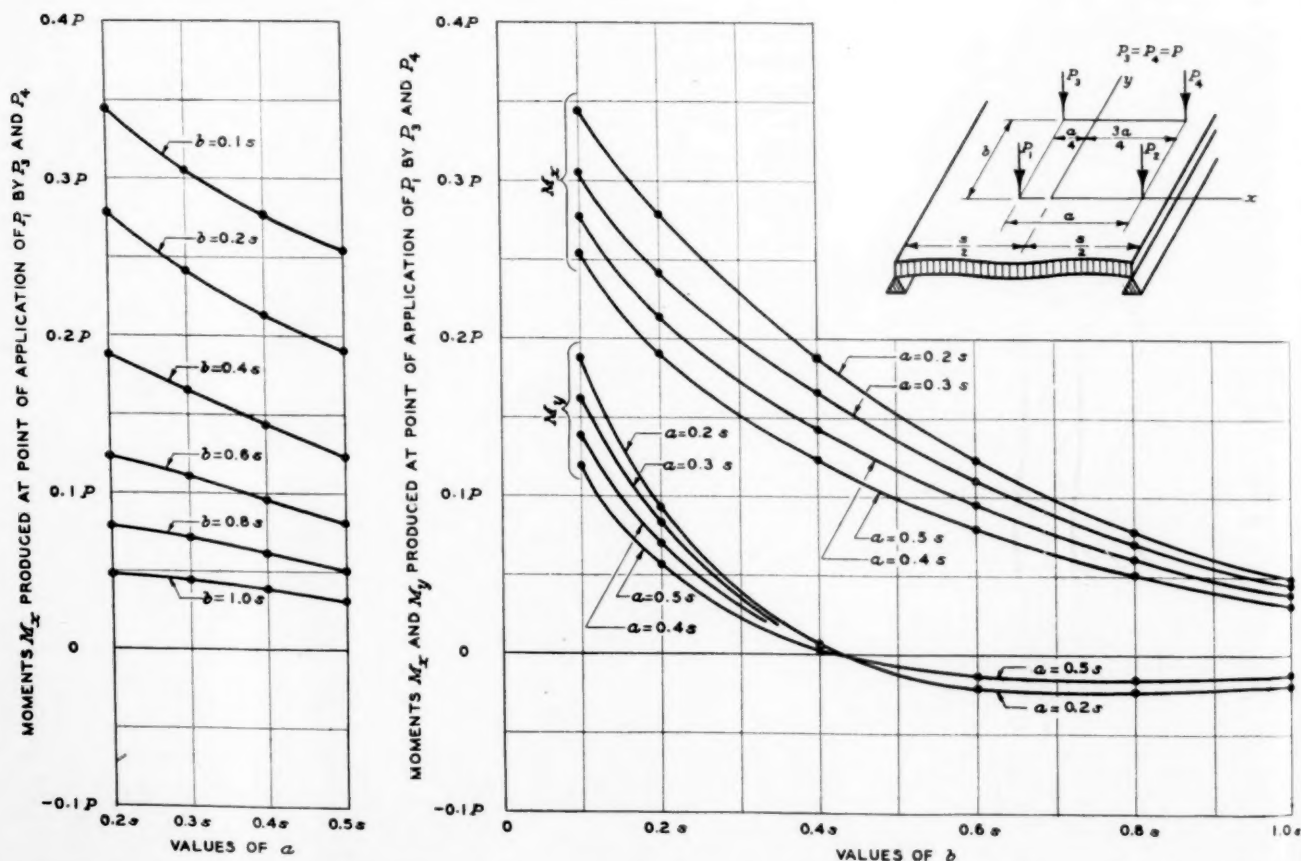

FIGURE 15.—BENDING MOMENTS PRODUCED AT POINT OF APPLICATION OF P_1 BY TWO LOADS, $P_3 = P$ AND $P_4 = P$ (FROM EQUATION 88 AND TABLE 6). POISSON'S RATIO, $\mu = 0.15$

One finds, furthermore,

$$\frac{dM}{du} = \sum_{1,2,\cdots}^{n} n\, C_n\, (\sin 2nu + \sin n(2u + a)) \quad (82)$$

which becomes zero when $u = \frac{\pi}{2} - \frac{a}{4}$, or $v = \frac{a}{4}$. It is concluded that M_x or M_y, respectively, reaches an extreme value when $r = \frac{a}{4}$, and that this value is a maximum when M in equation 80 is positive for all values of x between 0 and π. That is, the rule by which two equal loads are placed on a beam so as to produce a maximum moment, and which was found to apply to P_1 and P_2, applies also to P_3 and P_4.

The y-axis is now moved back to the center-line of the slab, and the span is assumed to have any value, s. The two loads $P_3 = P$ and $P_4 = P$ are placed as shown in Figure 15. For these two loads equations 44 and 45 give equal values of A, but different values of B, which will be denoted by B_3 and B_4, respectively. One finds

$$A = \cosh \frac{\pi b}{s} + \cos \frac{\pi a}{2s} \quad (83)$$

$$B_3 = \cosh \frac{\pi b}{s} - 1 \quad (84)$$

$$B_4 = \cosh \frac{\pi b}{s} - \cos \frac{\pi a}{s} \quad (85)$$

The moments produced by the two loads, $P_3 = P$ and $P_4 = P$, then may be expressed as follows, by use of equations 51 and 54:

$$\left.\begin{array}{c} M_x \\ M_y \end{array}\right| = \frac{(1+\mu)P}{8\pi} \log_e \frac{A^2}{B_3 B_4} \pm$$
$$\frac{(1-\mu)Pb}{8s} \sinh \frac{\pi b}{s}\left(\frac{1}{B_3} + \frac{1}{B_4} - \frac{2}{A}\right) \quad (86)$$

$$M_{xy} = -\frac{(1-\mu)Pb}{8s}\frac{\sin\frac{\pi a}{s}}{B_4} \quad (87)$$

or, with $\mu = 0.15$,

$$\left.\begin{array}{c} M_x \\ M_y \end{array}\right| = 0.10536\, P \log_{10}\frac{A^2}{B_3 B_4} \pm$$
$$0.10625\frac{Pb}{s}\sinh\frac{\pi b}{s}\left(\frac{1}{B_3} + \frac{1}{B_4} - \frac{2}{A}\right) \quad (88)$$

$$M_{xy} = -0.10625\frac{Pb}{s}\frac{\sin\frac{\pi a}{s}}{B_4} \quad (89)$$

Table 6 contains values computed from equations 88 and 89 with use of equations 83, 84, and 85. Figure 15 shows curves representing equation 88.

A comparison of equations 87 and 76 shows that the twisting moment M_{xy} produced at the point $-\frac{a}{4}$, 0, by the two loads P at the points $-\frac{a}{4}$, b and $\frac{3a}{4}$, b, is equal to the twisting moment M'_{xy} produced at the point 0, 0 by a single load P at point $\frac{a}{2}$, $\frac{b}{2}$. Figures 13 and 14,

therefore, supply the necessary information about the twisting moments produced by P_3 and P_4.

COMBINED EFFECTS OF FOUR LOADS

To produce the greatest possible bending moments M_x and M_y at the point of application of P_1, the four loads, P_1, P_2, P_3, and P_4, each equal to P, are placed as shown in Figure 16. The combined effects of P_1 and P_2 are given in equations 71 and 72 and in Table 4, in conjunction with equations 60 and 61 and Table 1. The combined effects of P_3 and P_4 are defined by equations 83 to 89 and are given in Table 6. By adding the results, one finds the moments M_x, M_y, and M_{xy} produced at the point of application of P_1 by the combined action of the four loads. From these values one obtains the principal moments M_1 and M_2, that is, the greatest bending moment and the smallest bending moment at the particular point, and also the angle ψ between the x-axis and the direction of M_1, by the following formulas, which are analogous to those applying to a plane state of stresses:

$$\left.\begin{array}{c} M_1 \\ M_2 \end{array}\right| = \frac{M_x + M_y}{2} \pm \sqrt{\frac{(M_x - M_y)^2}{4} + M_{xy}^2} \quad (90)$$

$$\tan 2\psi = \frac{2M_{xy}}{M_x - M_y} \quad (91)$$

Table 6 contains values, for $P = 1$, of M_{xy} and of the amounts $M_x - M_{0x}$, $M_y - M_{0x}$, $M_1 - M_{0x}$, and $M_2 - M_{0x}$ which are to be added to M_{0x} (as given by equation 61 and in Table 1) in order to obtain the moments due to the four loads. The curves in Figures 16 and 17 show the values of $M_1 - M_{0x}$, $M_2 - M_{0x}$, and ψ for different values of a and b.

An examination of Figure 17 shows that the following formula applies as a crude approximation, giving values which are not too small, when $0.3s < a < 0.5s$, and $0.3s < b < s$:

$$\frac{M_1 - M_{0x}}{P} = \frac{0.4s}{2a + b} - 0.14 \quad (92)$$

Using this formula in conjunction with the roughly approximate formula, equation 66, one finds

$$M_1 = \frac{Ps}{2.32s + 8c} + \frac{0.4Ps}{2a + b} - 0.14P \quad (93)$$

DETERMINATION OF CHANGES CAUSED BY INTRODUCTION OF BEAMS IN DIRECTION OF x

Let the slab, extending indefinitely far in the directions of $+y$ and $-y$, be loaded by a force P at the point x, y_1 and by a force $-P$ (that is, an upward force P) at the point x, $2b_1 - y_1$ (where $b_1 > y_1$). The deflections, z, and bending moments, M_x and M_y, produced by the two loads at the line $y = b_1$ will neutralize each other, so that at this line one finds $z = \Delta z = 0$. The part of the slab for which $y < b_1$, therefore, behaves as if the slab had a simply supported edge at $y = b_1$. Likewise,[18] if one introduces a set of loads $+P$ at the points $x = x_1$, $y = y_1 + 2nl$, and loads $-P$ at the points $x = x_1$, $y = 2b_1 - y_1 + 2nl$, with $n = 0, \pm 1, \pm 2, \ldots$, the part of the slab between the lines $y = b_1$ and $y = b_1 - l$ will act as a rectangular slab which has simply supported edges

---

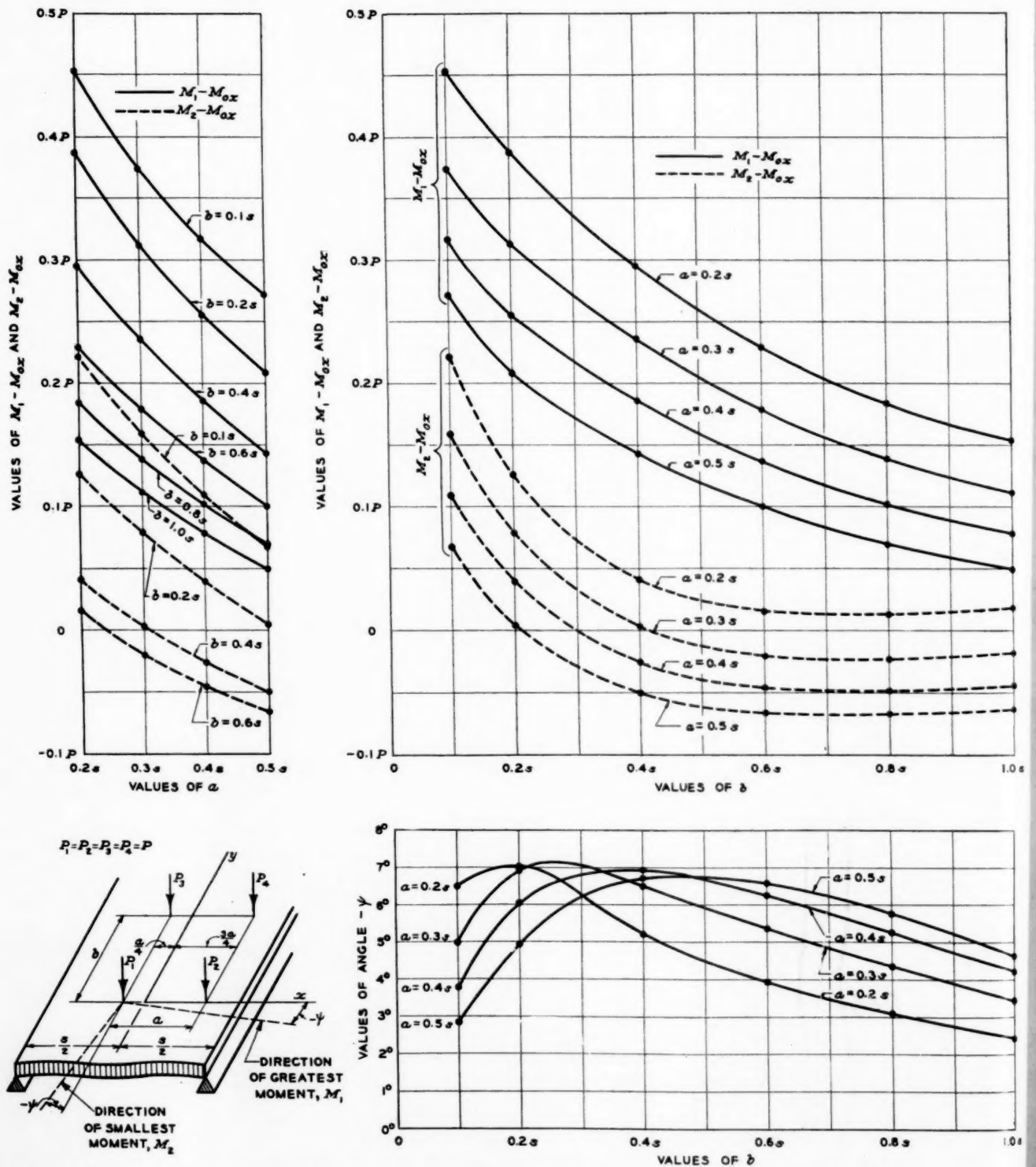[18] A. Nádai, Die elastischen Platten, 1925, p. 84.

FIGURE 16.—COMBINED EFFECTS OF FOUR LOADS. AMOUNTS TO BE ADDED TO M_{ox} TO OBTAIN PRINCIPAL MOMENTS M_1 AND M_2, PRODUCED AT POINT OF APPLICATION OF P_1 BY JOINT ACTION OF FOUR LOADS, P_1, P_2, P_3, AND P_4, EACH EQUAL TO P. ANGLES BETWEEN x-AXIS AND M_1. (FROM EQUATIONS 60, 72, AND 83 TO 91, AND TABLE 6.) POISSON'S RATIO, $\mu=0.15$
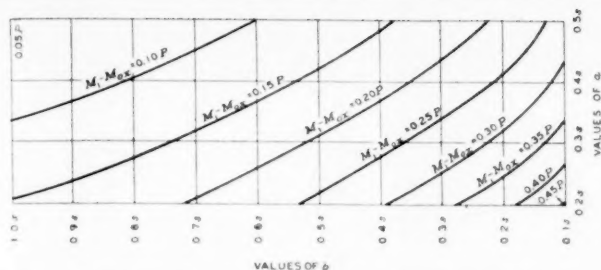
FIGURE 17.—COMBINED EFFECTS OF FOUR LOADS. CURVES FOR CONSTANT VALUES OF $M_1 - M_{0x}$, DETERMINED FROM FIGURE 16. POISSON'S RATIO, $\mu = 0.15$.

TABLE 6.—*Bending moments M_x and M_y produced at point $-\frac{a}{4}$, 0 by two loads, $P=1$, at points $-\frac{a}{4}$, b and $\frac{3a}{4}$, b, computed from equations 83, 84, 85, and 88, and represented graphically in Figure 15. Twisting moments M_{xy} produced at the same point by the same two loads, or by these loads in conjunction with P_1 and P_2, computed from equations 85 and 89. Amounts $M_x - M_{0x}$, $M_y - M_{0x}$, $M_1 - M_{0x}$, and $M_2 - M_{0x}$ to be added to M_{0x} to obtain the moments produced at point $-\frac{a}{4}$, 0 by the combined action of four loads, $P=1$, applied as shown in Figure 16, M_1 and M_2 being the principal moments at the point. Angle ψ between x-axis and direction of M_1. The values of $M_1 - M_{0x}$, $M_2 - M_{0x}$, and ψ are computed from equations 60, 72, and 83 to 91, and are represented graphically in Figures 16 and 17. Poisson's ratio, $\mu = 0.15$*

| | | From two loads | | | From four loads | | | | |
$\frac{a}{s}$	$\frac{b}{s}$	M_x	M_y	$-M_{xy}$	$\frac{M_x-}{M_{0x}}$	$\frac{M_y-}{M_{0x}}$	$\frac{M_1-}{M_{0x}}$	$\frac{M_2-}{M_{0x}}$	$-\psi$
0.2	0.1	0.34483	0.18703	0.02594	0.45003	0.22459	0.45297	0.22165	6°29′
	.2	.27823	.09281	.03163	.38343	.13037	.38733	.12647	7 1
	.4	.18788	.00566	.02292	.29308	.04322	.29517	.04113	5 12
	.6	.12318	−.02030	.01464	.22838	.01726	.22939	.01625	3 57
	.8	.07838	−.02348	.00925	.18358	.01408	.18408	.01358	3 7
	1.0	.04864	−.01934	.00579	.15384	.01822	.15408	.01798	2 26
.3	.1	.30536	.16128	.01861	.37250	.16078	.37412	.15916	4 59
	.2	.24195	.08321	.02790	.30909	.08271	.31248	.07932	6 55
	.4	.16583	.00691	.02622	.23297	.00641	.23597	.00341	6 31
	.6	.11039	−.01767	.01854	.17753	−.01817	.17927	−.01991	5 22
	.8	.07074	−.02106	.01222	.13788	−.02156	.13881	−.02249	4 22
	1.0	.04405	−.01747	.00781	.11119	−.01797	.11166	−.01844	3 27
.4	.1	.27690	.13864	.01364	.31634	.11044	.31724	.10954	3 46
	.2	.21347	.07023	.02258	.25291	.04203	.25530	.03964	6 3
	.4	.14361	.00603	.02542	.18305	−.02217	.18615	−.02527	6 57
	.6	.09563	−.01521	.01981	.13507	−.04341	.13724	−.04558	6 16
	.8	.06138	−.01824	.01369	.10082	−.04644	.10208	−.04770	5 16
	1.0	.03825	−.01517	.00896	.07769	−.04337	.07835	−.04403	4 13
.5	.1	.25423	.11909	.01012	.27146	.06868	.27196	.06818	2 51
	.2	.19030	.05674	.01765	.20753	.00633	.20907	.00479	4 59
	.4	.12297	.00339	.02238	.14020	−.04702	.14284	−.04966	6 43
	.6	.08037	−.01327	.01892	.09760	−.06368	.09979	−.06587	6 36
	.8	.05113	−.01535	.01368	.06836	−.06576	.06974	−.06714	5 46
	1.0	.03171	−.01261	.00917	.04894	−.06302	.04969	−.06377	4 39

at $x = \pm \frac{s}{2}$ and at $y = b_1$ and $y = b_1 - l$, and which is loaded by the force P at the point x_1, y_1. This equivalence of two cases leads to a simple determination of the action of the rectangular slab by use of the results found for the slab extending infinitely far in the directions of x and y.

As the first example, consider a slab which has simply supported edges at $x = \pm \frac{s}{2}$ and at $y = \frac{s}{2}$, and which extends infinitely far in the direction of $-y$. Let this slab be loaded by a force P at the point 0, 0. The slab extending infinitely far also in the direction of $+y$ then

is to be loaded by the additional force $-P$ at the point $x=0$, $y = 2b_1 - y_1 = s$. Values stated in the first section of Table 5, then give at the point 0, 0:

$$M_x = M_{0x} - 0.0263P$$

$$M_y = M_{0y} + 0.0105P$$

As a second example, consider a square slab loaded at the center. With $b_1 = \frac{s}{2}$, $l = s$, the loads P are introduced at the points $x = 0$, $y = 0$, $\pm 2s$, $\pm 4s$, . . . and the loads $-P$ are introduced at the points $x=0$, $y = \pm s$, $\pm 3s$, ... Then one finds at point 0, 0, by use of Table 5 and equation 62:

$$M_x = M_{0x} + 2(-0.0263 + 0.019 - 0.0001 + . . .)P$$

$$= M_{0x} - 0.0490P,$$

$$M_y = (M_{0x} - 0.0676P) + 2(0.0105 - 0.0013 +$$
$$0.0001 - . . .)P$$

$$= M_{0x} - 0.0490P.$$

The equality of the two moments, so determined, is noted. They should be equal since the slab is square.

EFFECTS OF CHANGING FROM SIMPLY SUPPORTED EDGES TO FIXED EDGES INVESTIGATED

A rectangular slab is considered which has simply supported edges at $x = \pm \frac{s}{2}$ and $y = \pm \frac{l}{2}$, and is loaded by a single force P at the center, point 0, 0. By introducing the symbols,

$$\omega_n = \frac{n\pi}{l}, \quad \alpha_n = \frac{\omega_n s}{2} = \frac{n\pi s}{2l}, \\ \text{where } n = 1, 3, 5, \cdots \quad \Big\} \text{------(94)}$$

one may show that the following formula expresses the deflection of this slab at the point x, y when $x \geqq 0$:

$$z = \frac{Pl^2}{2\pi^3 N} \sum_{1,3,5,\cdots}^{n} \frac{\cos \omega_n y}{n^3} \Big[\Big(\tanh \alpha_n - \frac{\alpha_n}{\cosh^2 \alpha_n} \Big) \cosh \omega_n x$$
$$- \omega_n x \tanh \alpha_n \sinh \omega_n x - \sinh \omega_n x + \omega_n x \cosh \omega_n x \Big]. (95)$$

To verify this formula, one may begin by observing that $z = 0$ when $x = \frac{s}{2}$ (giving $\omega_n x = \alpha_n$) and when $y = \pm \frac{l}{2}$. One finds

$$\frac{\partial z}{\partial x} = \frac{Pl}{2\pi^2 N} \sum_{1,3,5,\cdots}^{n} \frac{\cos \omega_n y}{n^2} \Big[\omega_n x \sinh \omega_n x$$
$$- \frac{\alpha_n}{\cosh^2 \alpha_n} \sinh \omega_n x - \omega_n x \tanh \alpha_n \cosh \omega_n x \Big] - (96)$$

which becomes zero when $x = 0$. By further differentiations one finds

$$\Delta z = \frac{P}{\pi N} \sum_{1,3,5,\cdots}^{n} \frac{\cos \omega_n y}{n} \Big[-\tanh \alpha_n \cosh \omega_n x + \sinh \omega_n x \Big]. (97)$$

which becomes zero when $x = \frac{s}{2}$ or $y = \pm \frac{l}{2}$. The vertical shear in a section parallel to the y-axis becomes, according to equation 17,

$$V_z = -N \frac{\partial \Delta z}{\partial x} = -\frac{P}{l} \sum_{1,3,5,\cdots}^{n} \cos \omega_n y \left[\cosh \omega_n x - \tanh \alpha_n \sinh \omega_n x \right] \quad (98)$$

When $x = 0$, this series assumes the divergent form,

$$V_z = -\frac{P}{l} \sum_{1,3,5,\cdots}^{n} \cos \frac{n \pi y}{l} \quad (99)$$

By comparing this equation with the expression for V_y in equation 29, it is seen that equation 99 expresses the fact that the boundary condition in the section $x = 0$, resulting from the presence of the concentrated load P at point 0, 0 is satisfied. By further differentiations of equation 97 one finds $\Delta^2 z = 0$. Thus, the function z in equation 95 satisfies the equation of flexure as well as all the conditions of the boundary.

The slope at the edge $x = \frac{s}{2}$ is of particular interest. Equation 96 gives at this line

$$\frac{\partial z}{\partial x} = -\frac{Pl}{2 \pi^2 N} \sum_{1,3,5,\cdots}^{n} \frac{\cos \omega_n y}{n^2} \frac{\alpha_n \sinh \alpha_n}{\cosh^2 \alpha_n} \quad (100)$$

Consider now the function,

$$z_1 = -\frac{Pl^2}{\pi^3 N} \sum_{1,3,5,\cdots}^{n} \frac{\cos \omega_n y}{n^3} \frac{\alpha_n \tanh \alpha_n}{\sinh 2\alpha_n + 2\alpha_n} \left[\alpha_n \tanh \alpha_n \cosh \omega_n x - \omega_n x \sinh \omega_n x \right] \quad (101)$$

This function is found to have the following properties:

At $y = \pm \frac{l}{2}$: $z_1 = \Delta z_1 = 0$.

At $x = 0$: $\frac{\partial z_1}{\partial x} = 0$, $V_z = -N \frac{\partial \Delta z_1}{\partial x} = 0$.

At $x = \frac{s}{2}$: $z_1 = 0$, $\frac{\partial z_1}{\partial x} = -\frac{\partial z}{\partial x}$ (equation 100).

At all points: $\Delta^2 z_1 = 0$.

It follows that the function $z' = z + z_1$ represents the deflection (for $x > 0$) of a rectangular slab which has simply supported edges at $y = \pm \frac{l}{2}$ and fixed edges at $x = \pm \frac{s}{2}$, and which is loaded by the force P at the point 0, 0. That is, z_1 represents the change of deflection caused by fixing the two edges parallel to the y-axis.

The corresponding changes of the moments in the section $x = 0$ are then expressed as follows, by use of equations 11 and 12:

$$M'_x - M_x = N \left[-\frac{\partial^2 z_1}{\partial x^2} - \mu \frac{\partial^2 z_1}{\partial y^2} \right]_{x=0}$$

$$= \frac{Ps}{2l} \sum_{1,3,5,\cdots}^{n} \frac{\cos \omega_n y}{\sinh 2} \frac{\tanh \alpha_n}{\alpha_n + 2\alpha_n} [(1 - \mu)\alpha_n \tanh \alpha_n - 2] \quad (102)$$

$$M'_y - M_y = N \left[-\frac{\partial^2 z_1}{\partial y^2} - \mu \frac{\partial^2 z_1}{\partial x^2} \right]_{x=0}$$

$$= \frac{Ps}{2l} \sum_{1,3,5,\cdots}^{n} \frac{\cos \omega_n y}{\sinh 2} \frac{\tanh \alpha_n}{\alpha_n + 2\alpha_n} [-(1 - \mu)\alpha_n \tanh \alpha_n - 2\mu] \quad (103)$$

The values stated in Table 7 have been computed from equations 102 and 103 with $\mu = 0.15$ and $l = 2.5 \pi s = 7.854 s$. The value of l is so large that changing it to infinity would make no noticeable difference. The results are represented graphically by the curves in the lower part of Figure 9. The curves for M'_x and M'_y in the upper part of Figure 9 were constructed from the curves for M_x and M_y by laying off intercepts equal to $M'_x - M_x$ and $M'_y - M_y$.

From the values given in the table for point $x = y = 0$, one finds by use of equation 60:

$$M'_{0x} = M_{0x} - 0.0699P \quad (104)$$

$$M'_{0y} = M_{0x} - 0.06764P - 0.03863P = M_{0x} - 0.1063P \quad (105)$$

These formulas explain the two scales farthest to the right in Figure 6.

TABLE 7.—*Changes, $M'_x - M_x$ and $M'_y - M_y$, of the bending moments at the center-line of the slab, caused by change from simply supported edges to fixed edges, when the slab is loaded by the force $P = 1$ at point 0, 0. Values computed from equations 102 and 103, and shown graphically in Figure 9. Poisson's ratio, $\mu = 0.15$*

$\frac{y}{s}$	$M'_x - M_x$	$M'_y - M_y$	$\frac{y}{s}$	$M'_x - M_x$	$M'_y - M_y$
0	−0.06994	−0.03863	1.0	−0.0248	0.0059
.2	−.06755	−.0323	1.5	−.00764	.00386
.4	−.0602	−.0181	2	−.00198	.00129
.6	−.0489	−.0048			

SLAB CANTILEVERED FROM A SINGLE FIXED EDGE INVESTIGATED

The slab shown in Figure 18 has a fixed edge along the y-axis, and is assumed to cover one-half of the xy-plane, the part for which x is positive. Consider the bending moment M_x produced at the point 0, 0 by a load $P = 1$ at the point x, y. The locus of a point with the three rectangular coordinates x, y, M_x is the influence surface for M_x. It is well known that any influence diagram may be obtained as a deflection diagram by introducing the proper discontinuity at the point under investigation. In applying this principle to the present case, one is to determine a surface with coordinates x, y, z, so that the function z satisfies the following conditions: It is required, first, that the equation of flexure
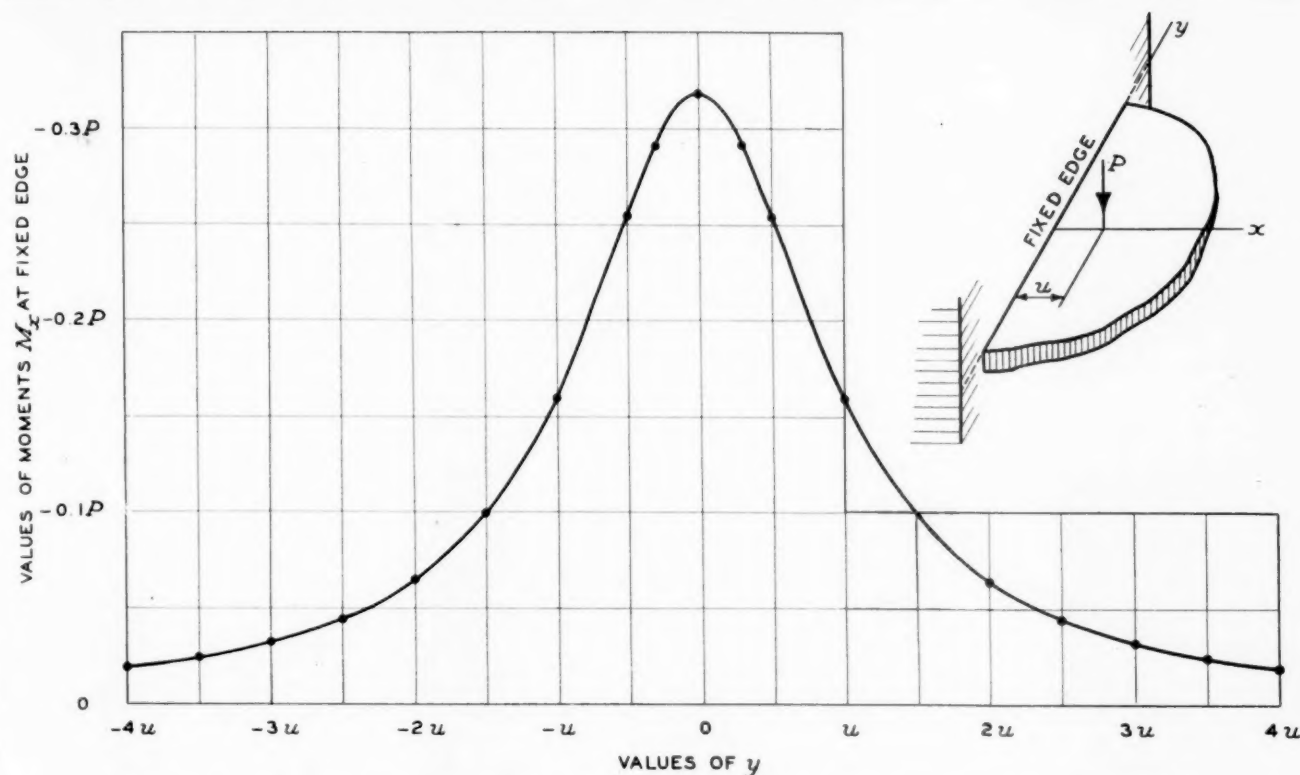
FIGURE 18.—BENDING MOMENTS AT FIXED EDGE OF LARGE SLAB (FROM EQUATION 110 AND TABLE 8)

$\Delta^2 z = 0$, be satisfied at all points except at the point 0, 0, where the function has a singularity; secondly, that $z = \dfrac{\partial z}{\partial x} = 0$ at the edge $x = 0$, except at the point 0, 0; thirdly, that z and Δz shall converge toward zero when x or y increases indefinitely; and fourthly, that the singularity at the point 0, 0 shall represent a proper concentration of slope at the particular point.

One may think of this concentration of a slope as one thinks of the concentration of a force: The distributed force $p = p(y)$ represents a total load $P = \int p \, dy$; by changing the function p gradually, but maintaining the value of the integral, the distributed force may be changed into the concentrated load. The function $\dfrac{\partial z}{\partial x}$ may be concentrated by gradual change in the same manner as the function p.

A function z of the following form is found to satisfy the requirements:

$$z = \frac{kx^2}{x^2 + y^2} \quad\text{----------(106)}$$

where k is a constant. A simple method of determining this constant is by noting that a distributed load, one unit per unit of length, on the line $x = 1$, produces a moment $M_x = -1$ at the edge. That is,

$$-1 = \int_{-\infty}^{\infty} \frac{k \, dy}{1 + y^2} = k\pi, \text{ or, } k = -\frac{1}{\pi} \quad\text{-----(107)}$$

Since z in equation 106 is interpreted as equal to the desired moment M_z at the point 0, 0, one finds

$$M_z = -\frac{x^2}{\pi(x^2 + y^2)} \quad\text{-----------(108)}$$

or, in terms of the angle θ from the x-axis to the radius vector,

$$M_x = -\frac{1}{\pi}\cos^2\theta \quad\text{-----------(109)}$$

The result expressed in equation 108 may be restated as follows: A load P at the point u, 0 produces a moment diagram at the edge with the equation,

$$M_x = -\frac{P}{\pi}\frac{1}{1 + \dfrac{y^2}{u^2}} \quad\text{-----------(110)}$$

Table 8 and Figure 18 show values computed from this equation.

TABLE 8.—*Moments M_x at fixed edge in Figure 18 when $P = 1$, computed from equation 110*

$\dfrac{y}{u}$	$-M_x$	$\dfrac{y}{u}$	$-M_x$
0	0.3183	2.0	0.0637
.3	.2920	2.5	.0439
.5	.2546	3.0	.0318
1.0	.1592	3.5	.0240
1.5	.0979	4.0	.0187

It is of some interest to know the bending moment M_z produced at point 0, 0 in Figure 18 when the load P is distributed uniformly over a circle with diameter c tangent to the edge at point 0, 0. Equation 109 gives

$$M_x = -\int_{-\frac{\pi}{2}}^{\frac{\pi}{2}} d\theta \int_0^{c\cos\theta} \frac{4Pr \, dr}{\pi c^2} \frac{\cos^2\theta}{\pi},$$

or,

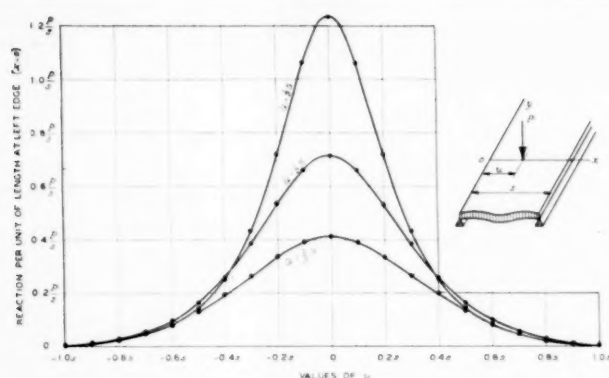$$M_x = -\frac{3P}{4\pi} \quad\text{-----------(111)}$$

FIGURE 19.—REACTIONS AT LEFT EDGE (FROM EQUATION 115 AND TABLE 9). POISSON'S RATIO, $\mu = 0.15$

This moment is three-fourths of the moment produced when the load P is concentrated at the center of the circle.

REACTIONS DETERMINED

Consider the case shown in Figure 19. The y-axis is at the left edge. The two edges are simply supported, and the slab extends infinitely far in the directions of $+y$ and $-y$. The load P is applied at the point u, 0. From equations 17, 43 to 46, and 52, and by consideration of the changed position of the y-axis, one finds the shear V_x and the twisting moment M_{xy} at the left edge,

$$V_x = \frac{P}{2s} \frac{\sin \frac{\pi u}{s}}{\cosh \frac{\pi y}{s} - \cos \frac{\pi u}{s}} \quad (112)$$

$$M_{xy} = \frac{(1-\mu)Py}{4s} \frac{\sin \frac{\pi u}{s}}{\cosh \frac{\pi y}{s} - \cos \frac{\pi u}{s}} \quad (113)$$

According to equation 19 this combination of shears and twisting moments is equivalent to the vertical reaction,

$$R_x = V_x + \frac{\partial M_{xy}}{\partial y} = \frac{(3-\mu)P}{4s} \frac{\sin \frac{\pi u}{s}}{\cosh \frac{\pi y}{s} - \cos \frac{\pi u}{s}} \times$$

$$\left(1 - \frac{1-\mu}{3-\mu} \frac{\frac{\pi y}{s} \sinh \frac{\pi y}{s}}{\cosh \frac{\pi y}{s} - \cos \frac{\pi u}{s}} \right) \quad (114)$$

or, with $\mu = 0.15$,

$$R_x = 0.7125 \frac{P}{s} \frac{\sin \frac{\pi u}{s}}{\cosh \frac{\pi y}{s} - \cos \frac{\pi u}{s}} \times$$

$$\left(1 - 0.29825 \frac{\frac{\pi y}{s} \sinh \frac{\pi y}{s}}{\cosh \frac{\pi y}{s} - \cos \frac{\pi u}{s}} \right) \quad (115)$$

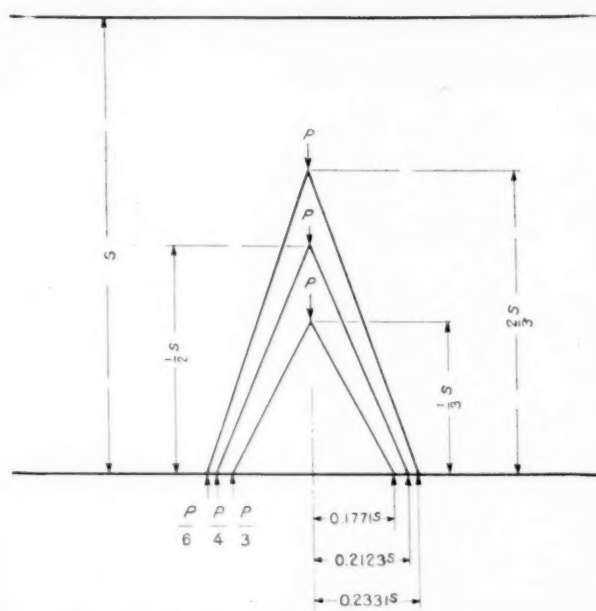Table 9 and Figure 19 show values computed from equation 115.

FIGURE 20.—POSITIONS OF RESULTANTS, EACH REPRESENTING LEFT HALF OR RIGHT HALF OF THE DIAGRAM OF REACTIONS, IN CASES SHOWN IN FIGURE 19 (FROM EQUATION 116). POISSON'S RATIO, $\mu = 0.15$

TABLE 9.—*Reactions R_x produced at the left edge by a load $P = 1$ on the x-axis at the distance u from the edge, computed from equation 115, and represented graphically in Figure 19. Poisson's ratio, $\mu = 0.15$*

$\frac{y}{s}$	Reaction R_x			$\frac{y}{s}$	Reaction R_x		
	$u = \frac{1}{3}s$	$u = \frac{1}{2}s$	$u = \frac{2}{3}s$		$u = \frac{1}{3}s$	$u = \frac{1}{2}s$	$u = \frac{2}{3}s$
0	1.2340	0.7125	0.4113	0.7	0.0427	0.056	0.0515
.1	1.0612	.659	.3904	.8	.0211	.030	.0290
.2	.7200	.530	.3354	.9	.0085	.014	.0144
.3	.4336	.382	.2636	1.0	.0014	.004	.0054
.4	.2503	.256	.1923	1.07		.000	
.5	.1423	.162	.1315	1.1		−.001	
.6	.0795	.098	.0849				

For the purpose of computing bending moments in the supporting beams, it is of interest to know the position of the resultant force representing the right half of each of the symmetrical diagrams in Figure 19. The distance, y_R from the point 0, 0 to this resultant is defined by the equation of moments,

$$y_R \int_0^\infty R_x \, dy = \int_0^\infty R_x y \, dy \quad (116)$$

The integral on the left side of this equation becomes in the three cases $\frac{P}{3}$, $\frac{P}{4}$, and $\frac{P}{6}$, respectively. The integral on the right side was determined in each of the three cases by numerical integration. By this method the three distances y_R shown in Figure 20 were obtained. One may interpret these results by saying that the resultant of the whole reaction is resolved in each case into two sub-resultants, each representing one-half of the diagram, and located as shown in Figure 20. An examination of the values given in Figure 20 shows that the following formula applies as a rough approximation:
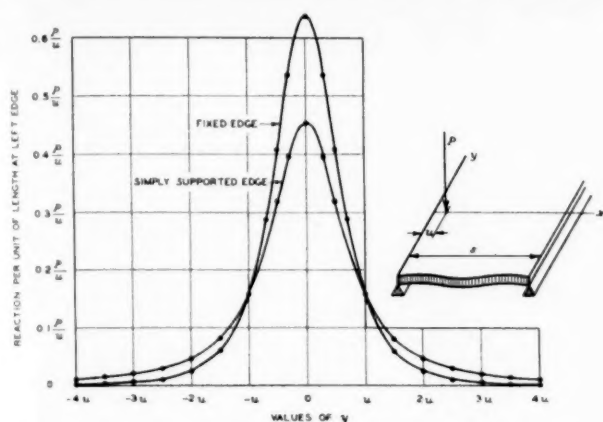
$$y_R = 0.3 \sqrt{us} \quad (117)$$

FIGURE 21.—REACTIONS PRODUCED BY LOAD CLOSE TO EDGE (FROM EQUATIONS 119 AND 120, AND TABLE 10) IN CASE OF SIMPLY SUPPORTED EDGE, POISSON'S RATIO, $\mu=0.15$

When the distance u from the edge to the load becomes small in comparison with the span, one may simplify equation 114 by substituting,

$$\sin\frac{\pi u}{s}=\frac{\pi u}{s},\ \sinh\frac{\pi y}{s}=\frac{\pi y}{s},\ \cosh\frac{\pi y}{s}-\cos\frac{\pi u}{s}=\frac{\pi^2}{2s^2}(y^2+u^2).$$

Then one finds

$$R_z=\frac{P}{2\pi}\frac{u}{u^2+y^2}\left(1+\mu+2(1-\mu)\frac{u^2}{u^2+y^2}\right)\quad(118)$$

or, with $\mu=0.15$,

$$R_z=0.1830\frac{P}{u}\frac{1}{1+\frac{y^2}{u^2}}\left(1+\frac{1.4783}{1+\frac{y^2}{u^2}}\right)\quad(119)$$

When the edge is fixed, one finds, by a procedure similar to that which led to equation 110,

$$R_z=\frac{2P}{\pi u}\frac{1}{\left(1+\frac{y^2}{u^2}\right)^2}=\frac{P}{u}\frac{0.6366}{\left(1+\frac{y^2}{u^2}\right)^2}\quad(120)$$

Table 10 and Figure 21 show results computed from equations 119 and 120.

If x is substituted for u in equations 118 to 120, these equations may be interpreted as defining the reaction R_z produced at point 0, 0 by a load P at point x,y. In terms of polar coordinates, with $x=r\cos\theta$, $y=r\sin\theta$, one finds then at point 0, 0 at the simply supported edge

$$R_z=\frac{P\cos\theta}{2\pi r}(1+\mu+2(1-\mu)\cos^2\theta)\quad(121)$$

TABLE 10.—*Reactions R_z produced at the left edge by a load $P=1$ on the x-axis at a small distance u from the edge, computed from equations 119 and 120, and represented graphically in Figure 21. In case of a simply supported edge, Poisson's ratio, $\mu=0.15$*

$\frac{y}{u}$	Values of R_z		$\frac{y}{u}$	Values of R_z	
	Simply supported edge	Fixed edge		Simply supported edge	Fixed edge
0	0.4535	0.6366	2.0	0.0474	0.0255
.3	.3956	.5358	2.5	.0304	.0121
.5	.3195	.4074	3.0	.0210	.0064
.7	----	.2867	3.5	.0154	.0036
1.0	.1591	.1592	4.0	.0117	.0022
1.5	.0819	.0603			

and at point 0, 0 of the fixed edge

$$R_z=\frac{2P}{\pi r}\cos^3\theta\quad(122)$$

One may use these formulas to determine the reaction per unit of length produced at point 0, 0 when the load P is distributed uniformly over the area of a small circle with diameter c, tangent to the edge at point 0, 0. By integrating over the area in the same manner as in deriving equation 111, one finds at point 0, 0 of the simply supported edge

$$R_z=\frac{5-\mu}{2}\frac{P}{\pi c}\quad(123)$$

and at point 0, 0 of the fixed edge

$$R_z=\frac{3P}{\pi c}\quad(124)$$

It is noted that $\frac{P}{\pi c}$ is the value that would be obtained if the force were distributed uniformly over the length of the circumference of the circle. At the fixed edge the twisting moments are zero, and R_z is the same as the shear V_z. At the simply supported edge, on the other hand, the presence of the twisting moments cause R_z in equation 123 to be larger than the shear V_z at the same point. One finds at point 0, 0

$$V_z=\frac{2P}{\pi c}\quad(125)$$

That is, the shear V_z at point 0, 0 is twice the value that would be found by distributing the load uniformly over the circumference of the circle.

ROAD PUBLICATIONS OF BUREAU OF PUBLIC ROADS

ANNUAL REPORTS

Report of the Chief of the Bureau of Public Roads, 1924.
Report of the Chief of the Bureau of Public Roads, 1925.
Report of the Chief of the Bureau of Public Roads, 1927.
Report of the Chief of the Bureau of Public Roads, 1928.

DEPARTMENT BULLETINS

No. *136D. Highway Bonds.   20c.
220D. Road Models.
257D. Progress Report of Experiments in Dust Prevention and Road Preservation, 1914.
*314D. Methods for the Examination of Bituminous Road Materials.   10c.
*347D. Methods for the Determination of the Physical Properties of Road-Building Rock.   10c.
*370D. The Results of Physical Tests of Road-Building Rock.   15c.
386D. Public Road Mileage and Revenues in the Middle Atlantic States, 1914.
387D. Public Road Mileage and Revenues in the Southern States, 1914.
388D. Public Road Mileage and Revenues in the New England States, 1914.
390D. Public Road Mileage and Revenues in the United States, 1914.   A Summary.
407D. Progress Reports of Experiments in Dust Prevention and Road Preservation, 1915.
463D. Earth, Sand-Clay, and Gravel Roads.
*532D. The Expansion and Contraction of Concrete and Concrete Roads.   10c.
*583D. Reports on Experimental Convict Road Camp, Fulton County, Ga.   25c.
*660D. Highway Cost Keeping.   10c.
*670D. The Results of Physical Tests of Road-Building Rock in 1916 and 1917.
*691D. Typical Specifications for Bituminous Road Materials.   10c.
*724D. Drainage Methods and Foundations for County Roads.   20c.
1216D. Tentative Standard Methods of Sampling and Testing Highway Materials, adopted by the American Association of State Highway Officials and approved by the Secretary of Agriculture for use in connection with Federal-aid road construction.
1259D. Standard Specifications for Steel Highway Bridges, adopted by the American Association of State Highway Officials and approved by the Secretary of Agriculture for use in connection with Federal-aid road work.
1279D. Rural Highway Mileage, Income, and Expenditures 1921 and 1922.
1486D. Highway Bridge Location.

DEPARTMENT CIRCULARS

No. 94C. T. N. T. as a Blasting Explosive.
331C. Standard Specifications for Corrugated Metal Pipe Culverts.

TECHNICAL BULLETIN

No. 55. Highway Bridge Surveys.

MISCELLANEOUS CIRCULARS

No. 62M. Standards Governing Plans, Specifications, Contract Forms, and Estimates for Federal-Aid Highway Projects.
*93M. Direct Production Costs of Broken Stone.   25c.
*109M. Federal Legislation and Regulations Relating to the Improvement of Federal-Aid Roads and National-Forest Roads and Trails.   10c.

SEPARATE REPRINTS FROM THE YEARBOOK

No. 914Y. Highways and Highway Transportation.
937Y. Miscellaneous Agricultural Statistics.
1036Y. Road Work on Farm Outlets Needs Skill and Right Equipment.

TRANSPORTATION SURVEY REPORTS

Report of a Survey of Transportation on the State Highway System of Connecticut.
Report of a Survey of Transportation on the State Highway System of Ohio.
Report of a Survey of Transportation on the State Highways of Vermont.
Report of a Survey of Transportation on the State Highways of New Hampshire.
Report of a Plan of Highway Improvement in the Regional Area of Cleveland, Ohio.
Report of a Survey of Transportation on the State Highways of Pennsylvania.

REPRINTS FROM THE JOURNAL OF AGRICULTURAL RESEARCH

Vol. 5, No. 17, D– 2. Effect of Controllable Variables upon the Penetration Test for Asphalts and Asphalt Cements.
Vol. 5, No. 19, D– 3. Relation Between Properties of Hardness and Toughness of Road-Building Rock.
Vol. 5, No. 24, D– 6. A New Penetration Needle for Use in Testing Bituminous Materials.
Vol. 6, No. 6, D– 8. Tests of Three Large-Sized Reinforced-Concrete Slabs Under Concentrated Loading.
Vol. 11, No. 10, D–15. Tests of a Large-Sized Reinforced-Concrete Slab Subjected to Eccentric Concentrated Loads.

UNITED STATES DEPARTMENT OF AGRICULTURE
BUREAU OF PUBLIC ROADS
CURRENT STATUS OF FEDERAL AID ROAD CONSTRUCTION
AS OF
FEBRUARY 28,1930

STATE	COMPLETED M.LEAGE	UNDER CONSTRUCTION Estimated total cost	Federal aid allotted	MILEAGE Initial	Stage	Total	APPROVED FOR CONSTRUCTION Estimated total cost	Federal aid allotted	MILEAGE Initial	Stage	Total	BALANCE OF FEDERAL AID FUNDS AVAIL ABLE FOR NEW PROJECTS	STATE
Alabama	2,101.3	$ 2,463,825.46	$ 1,215,498.79	87.0	21.0	108.0	$ 705,675.44	$ 531,303.02	0.3	14.9	15.2	$ 3,448,250.28	Alabama
Arizona	810.3	3,000,859.26	2,245,723.42	144.5	121.2	265.7	392,830.31	189,199.40	19.2	8.2	27.4	2,177,991.65	Arizona
Arkansas	1,764.5	3,354,511.57	1,601,744.38	142.0	28.7	170.7						2,593,119.20	Arkansas
California	1,947.9	6,532,917.52	2,900,406.90	163.5	9.2	172.7	2,734,581.03	702,156.06	37.1	15.0	53.1	1,697,621.10	California
Colorado	1,164.6	4,295,267.20	2,279,728.65	168.9	30.3	199.2	759,039.51	371,406.23	12.7	8.7	41.4	2,222,617.24	Colorado
Connecticut	240.3	1,095,990.67	455,428.90	6.5		6.5	671,564.46	272,075.09	3.6		3.6	914,520.46	Connecticut
Delaware	249.3	601,315.95	222,917.99	16.5	5.5	16.5	290,965.00	125,521.00	9.4		9.4	286,085.19	Delaware
Florida	467.2	5,042,471.20	2,384,205.05	102.1	8.5	107.5	601,441.91	247,779.63	16.9		16.9	1,342,041.00	Florida
Georgia	2,721.1	1,131,914.96	536,760.13	38.2		46.7						4,004,075.66	Georgia
Idaho	1,197.6	705,460.50	426,310.70	55.7	24.1	79.8	67,760.98	41,076.63	8.5	3.7	12.3	1,420,447.00	Idaho
Illinois	2,034.5	15,137,362.22	6,576,755.85	430.1		430.1	528,000.00	264,000.00	18.3		18.3	5,777,748.00	Illinois
Indiana	1,344.0	7,509,407.02	3,525,586.95	233.1		233.1	374,724.44	178,170.00	11.9		11.9	1,944,445.43	Indiana
Iowa	3,130.6	818,396.20	343,538.63	15.1	18.5	33.6	4,594,049.99	2,034,098.01	30.7	138.8	169.5	35,944.84	Iowa
Kansas	2,685.5	5,986,177.15	2,467,043.79	128.1	15.7	143.8	872,186.00	415,836.68	34.0	11.0	45.0	1,949,575.68	Kansas
Kentucky	1,397.8	4,238,953.63	2,013,037.35	235.5	20.2	255.7						1,846,732.84	Kentucky
Louisiana	1,357.0	3,767,314.15	1,842,730.53	109.1	11.2	120.3	459,872.51	224,703.86	17.9	1.3	19.1	1,701,842.24	Louisiana
Maine	520.0	1,905,021.13	736,937.56	47.5		47.5	87,912.01	43,956.00	5.5		5.5	1,523,961.32	Maine
Maryland	630.7	1,428,486.90	598,781.99	58.0		58.0	130,449.50	65,224.75	5.9		5.9	563,879.16	Maryland
Massachusetts	655.7	2,119,194.97	659,992.62	26.1	19.8	26.1	694,763.28	209,735.99	14.5	10.9	14.6	2,219,518.11	Massachusetts
Michigan	1,615.9	9,046,446.10	3,892,960.50	209.5	85.3	229.1	865,000.00	284,258.31	17.8	132.9	20.7	2,124,005.15	Michigan
Minnesota	4,107.5	4,778,319.59	1,384,300.00	123.5		208.8	4,741,128.77	973,165.90	77.3		210.2	515,066.97	Minnesota
Mississippi	1,806.0	1,965,437.01	776,543.31	70.4	7.7	78.1	5,703,470.44	1,853,748.42	82.8	56.7	139.5	2,645,070.13	Mississippi
Missouri	2,401.9	6,308,907.59	2,432,631.76	96.4	70.7	167.1	604,529.91	604,529.91	66.8	36.3	123.1	764,117.91	Missouri
Montana	1,722.2	7,241,717.11	4,217,128.89	487.0	12.9	499.9	1,106,093.36					3,052,191.62	Montana
Nebraska	3,589.1	6,790,134.88	3,290,038.01	330.5	155.3	485.9	396,762.02	183,657.74	19.9	15.1	15.0	2,262,918.67	Nebraska
Nevada	1,141.7	1,151,431.44	1,013,967.88	120.4	79.2	199.6	199,537.41	177,377.82		26.6	26.5	760,317.95	Nevada
New Hampshire	350.6	414,924.02	111,495.00	5.4	2.1	7.5						449,183.35	New Hampshire
New Jersey	900.2	4,136,530.77	852,015.00	56.8		56.8	765,700.57	447,423.65	44.4	4.4	48.8	1,091,104.08	New Jersey
New Mexico	1,935.0	2,907,004.00	1,842,980.28	152.9		155.0	5,563,700.00	994,500.00	66.4		66.4	1,032,152.51	New Mexico
New York	2,458.1	17,382,217.76	3,661,205.00	244.8	2.1	244.8						6,428,902.56	New York
North Carolina	1,765.2	1,297,923.70	6,8,411.59	74.3	22.3	97.2	1,511,206.23	755,103.11	84.3	110.8	84.3	2,213,056.34	North Carolina
North Dakota	4,176.4	1,196,709.89	487,732.47	205.4	101.7	307.1	1,530,915.56	834,183.23	313.1	25.6	423.9	1,182,762.15	North Dakota
Ohio	2,170.7	12,587,959.21	3,725,535.17	208.2	18.3	226.5	6,136,324.21	1,869,648.41	98.0		123.6	2,347,040.36	Ohio
Oklahoma	1,849.0	3,134,520.06	1,419,128.91	104.3	29.9	134.2	1,075,101.20	459,795.00	16.1	35.8	51.9	1,312,499.09	Oklahoma
Oregon	1,147.7	2,647,469.16	1,397,155.00	176.9	56.2	233.1	1,460,053.10	884,609.48	35.0	19.4	55.4	736,650.76	Oregon
Pennsylvania	2,261.3	13,931,265.99	3,941,443.44	205.5	14.1	219.7	4,410,877.44	1,294,915.30	72.7		72.7	2,131,043.84	Pennsylvania
Rhode Island	184.8	1,361,818.65	395,609.58	18.5	24.1	18.5	222,628.47	57,000.00	.2	6.8	7.0	617,409.52	Rhode Island
South Carolina	1,895.0	1,036,943.61	1,054,207.62	86.6	127.5	110.7	291,479.62	160,313.76	46.6	27.2	73.9	1,335,995.59	South Carolina
South Dakota	3,426.4	3,704,890.94	2,004,141.05	417.2		544.9						1,044,848.43	South Dakota
Tennessee	1,243.3	1,708,518.59	735,475.82	63.5		63.5	417,314.69	208,657.33	11.3	12.5	23.8	2,355,065.74	Tennessee
Texas	6,635.9	12,960,099.01	5,375,011.99	385.6	121.3	506.9	2,243,963.71	680,611.57	103.7	15.0	118.7	3,906,982.08	Texas
Utah	988.9	605,195.18	393,789.85	25.8		25.9	437,737.07	320,561.68	21.8	8.1	29.9	721,066.76	Utah
Vermont	257.8	524,815.88	209,469.96	9.3	15.6	9.3	897,266.54	202,682.46	20.1	7.7	20.1	228,425.52	Vermont
Virginia	1,413.8	2,663,848.90	1,252,004.96	120.6	40.2	136.2	1,319,405.52	587,980.18	39.5		47.3	721,194.21	Virginia
Washington	903.9	3,437,056.44	1,321,000.00	75.5		115.7	54,575.94	29,300.00	2.0		2.0	1,331,467.47	Washington
West Virginia	707.3	3,376,854.53	1,204,271.77	81.0	12.5	93.5	328,379.17	159,090.53	7.4	6.1	13.5	647,149.16	West Virginia
Wisconsin	2,280.1	4,268,427.21	1,907,945.11	153.9	3.9	157.8						1,655,897.08	Wisconsin
Wyoming	1,757.1	1,333,730.81	862,873.64	118.6	24.3	142.9						950,312.95	Wyoming
Hawaii	39.5	402,261.10	137,426.62	6.6		6.6	562,688.38	247,259.61	16.6		16.6	1,439,289.16	Hawaii
TOTALS	83,074.3	207,908,134.89	84,643,705.46	6,843.1	1,361.0	8,204.1	56,296,021.89	20,326,935.75	1,551.4	760.5	2,311.9	85,570,583.31	TOTALS